Journal of Materials Chemistry A

REVIEW

View Article Online
View Journal | View Issue

Cite this: J. Mater. Chem. A, 2024, 12, 21531

Recent advances and perspectives of 1D/2D carbon materials for high-performance flexible zinc ion batteries

Qingqing Zheng, [a] Zewei Hu,[a] Liyang Liu,[a] Haiying Lu,[a] Xin Wang,[a] Yongpeng Lei, [a] Chao Han[b] and Weijie Li *[a]

Flexible zinc ion batteries (FZIBs) have garnered significant attention owing to their cost-effectiveness, environmental friendliness, excellent flexibility and advanced security. Nevertheless, the electrochemical performance of FZIBs, such as energy density and cycling life, has yet to be improved compared to that of conventional rigid zinc-ion batteries (ZIBs). Due to the excellent electrical conductivity and mechanical properties exhibited by advanced one or two dimensional (1D/2D) carbon materials, they are increasingly recognized to play a key role in constructing flexible electrodes and improving the capacity, energy density/power density of FZIBs. However, no review comprehensively summarizes the functions and advances of 1D/2D carbon materials in FZIBs to date. In this review, a comprehensive overview of the development background of 1D/2D carbon materials (carbon nanotubes, graphene, MXenes and carbon fiber), highlighting their great advantages and functions of applications in FZIBs is given. Detailed summaries of recent advancements and the current challenges of 1D/2D carbon materials for high-performance FZIBs along with promising strategies are provided. First, the essential requirements and challenges of FZIBs and the fundamental aspects of 1D/2D carbon materials, including the development background and the unique advantages of these 1D/2D carbon materials applied in FZIBs are summarized. Then, the latest developments of these 1D/2D materials in FZIBs, which could function as active materials, conductive networks, current collectors or Zn hosts in FZIBs are discussed. In addition, the application of 1D/2D carbon materials in separators and gel electrolytes is specially emphasized. Finally, the development prospect of 1D/2D carbon materials used in FZIBs is briefly discussed.

Received 27th May 2024
Accepted 11th July 2024

DOI: 10.1039/d4ta03650f

rsc.li/materials-a

1. Introduction

With the continuous progress of technology, the application of flexible electronics is becoming increasingly widespread.

[a]State Key Laboratory for Powder Metallurgy, Central South University, Changsha, 410083, China. E-mail: li-306@csu.edu.cn

[b]School of Materials Sciences and Engineering, Central South University, Changsha, 410083, China

Chao Han

Chao Han got his PhD degree from the University of Wollongong (Australia) and now works at Central South University. His research field is materials physics and chemistry including thermoelectrics, electrocatalysts, and batteries. He serves as Young Editors for Battery Energy at present.

Weijie Li

Wei-Jie Li obtained her PhD degree (2016) from the University of Wollongong, Australia. Then, she worked at the University of Wollongong as an associate research fellow and DECRA research fellow for 6 years. She is currently a research fellow at the State Key Laboratory for Powder Metallurgy, Central South University in China. Her current research interest is focused on developing energy storage systems with high energy density (including sodium ion batteries and aqueous batteries).

Examples include implantable electronic skins in medicine, wearable health monitoring systems, smart clothing, and flexible displays.[1–4] However, traditional energy storage devices, such as supercapacitors, are too large, heavy, and expensive to be compatible with flexible electronic devices.[5,6] Therefore, developing small, lightweight, low-cost, and fast-charging flexible energy storage devices is an important challenge for technological innovation in flexible electronics. Various studies have been conducted on flexible batteries, which could be an integral part of flexible electronic products.[7,8]

As a resource-rich metal in the world, zinc has attracted a lot of attention due to its cheap price, non-toxic and environmentally friendly nature, low redox potential (−0.76 V *versus* the standard hydrogen electrode (SHE)), and high theoretical capacity (820 mA h g^{-1} or 5855 mA h cm^{-3}).[9–12] Moreover, compared with traditional liquid electrolytes based on organic solvents, aqueous electrolytes display higher biocompatibility and environmental friendliness, and avoid safety concerns.[13,14] Thus, ZIBs are suitable for developing flexible batteries for flexible electronic products. However, the employment of aqueous electrolytes is not suitable in flexible batteries due to the potential liquid leakage under deformation.[15] In addition, aqueous electrolytes tend to induce the growth of zinc dendrites and the formation of soluble ZnO_2 on the zinc anode, which poison the cathode, resulting in rapid capacity attenuation.[16–18] Polymer/hydrogel electrolytes are becoming crucial in addressing specific challenges in flexible battery technology due to their relatively low water content. Furthermore, the formation of a solid–solid interface between the electrodes and polymer/hydrogel electrolytes, rather than a solid–liquid interface, significantly enhances the stability of the battery system.[19–21] This alteration mitigates the risks associated with dendrite formation and the degradation of cathode materials. However, polymer/hydrogel electrolytes usually possess low ionic conductivity and high interfacial resistance. Therefore, the batteries consisting of polymer/hydrogel electrolytes exhibit poor rate performance and high resistance.[22–24] In addition, conventional metal oxide cathodes suffer from inherently low conductivity, which hinders rapid electron transfer. Their mechanical instability also renders them unable to cope with repeated volume changes during the intercalation/deintercalation cycles.[13,25] Moreover, when these cathode materials are directly exposed to mild acid electrolytes, it typically leads to the dissolution of active materials, which accelerates the capacity loss.[26] Simultaneously, flexible zinc anodes require robust mechanical stability to ensure the preservation of electrochemical performance and structural integrity during deformation such as bending or stretching. However, flexible zinc anodes are often susceptible to mechanical damage or fatigue.[27,28] This problem could cause short circuits of batteries. Collectively, these challenges in both cathode and anode materials contribute to suboptimal zinc storage outcomes, manifesting in lower energy density and a restricted cycling life.

To tackle the mentioned challenges and pursue for the high-performance and excellent mechanical properties of FZIBs, it requires the utilization of flexible battery components (*e.g.*, cathodes, anodes and electrolytes).[29,30] Over the past decade, 1D/2D carbon materials have increasingly been applied in FZIBs owing to their superior electrical conductivity, mechanical properties, and adjustable porous structures.[31,32] These 1D materials include carbon nanotubes (CNTs), carbon fibers (CFs), and 2D materials include graphene and MXenes.[33,34] For example, Zhi *et al.*[35] explained the design principles and device performance of flexible fiber-based batteries. Hu *et al.*[36] introduced the design mechanisms of carbon nanotubes (CNTs), carbon fibers (CFs), and other carbon materials in flexible batteries based on thin films and fibers that can be bent. Moreover, previous reviews on FZIBs have primarily focused on gel electrolytes. For instance, He and colleagues reviewed recent advancements in polymer electrolytes, particularly focusing on the synthesis and characterization of gel electrolytes. Their work aimed to provide insights from laboratory research to commercialization.[37] Similarly, Li's team systematically discussed and evaluated the preparation methods of functional gel electrolytes for FZIBs from a fabrication perspective.[38] Zhang and colleagues introduced the latest research progress and rational design strategies of flexible quasi-solid-state ZIBs from the perspectives of mechanisms, design principles and applications.[39] However, until now, no review has comprehensively reported the progress of application of 1D/2D carbon materials in the cathodes, anodes, gel electrolytes and separators of FZIBs. With the attention to flexible electronics increasing, there is an urgent need for a systematic and timely review of the recent advancements in the use of 1D/2D carbon materials in FZIBs to provide potential directions for the next generation of FZIBs.

In this review, we aim to figure out the development background of 1D/2D carbon materials, highlighting their great advantages and functions of applications in FZIBs. Detailed summaries of recent advancements and the current challenges of 1D/2D carbon materials for high-performance FZIBs along

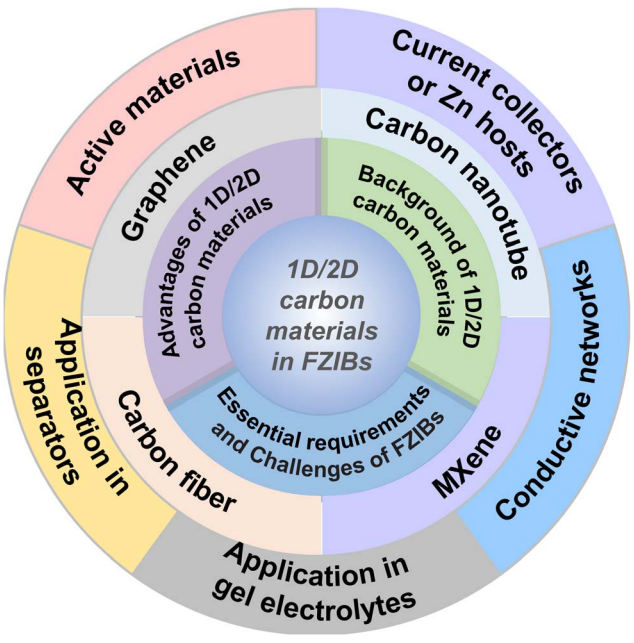

Fig. 1 Schematic depiction of the frame construction of this review.

with promising strategies are provided. As depicted in Fig. 1, this review begins by introducing the essential requirements and challenges of FZIBs. Currently summarizing the fundamental aspects of 1D/2D carbon materials (carbon nanotubes, graphene, MXenes and carbon fiber), including the development background and the unique advantages of these 1D/2D carbon materials applied in FZIBs. Then, the latest developments of these 1D/2D materials in FZIBs, which could function as active materials, conductive networks, current collectors or Zn hosts in FZIBs are discussed. In addition, the application of 1D/2D carbon materials in separators and gel electrolytes is specially emphasized. Finally, the development prospect of 1D/2D carbon materials used in FZIBs is briefly discussed. We hope to provide valuable suggestions for the research and development of 1D/2D carbon material applying in FZIBs through this review.

2. Fundamentals of 1D/2D carbon materials in FZIBs

2.1. Essential requirements and challenges of FZIBs

FZIBs represent an emerging field of energy storage technologies, particularly for applications requiring flexibility, such as wearable electronics, flexible displays, and medical implants.[40] FZIBs offer a viable alternative to traditional LIBs due to the plentiful supply of zinc in the world, low cost, and safety.[41] Nonetheless, their progress also faces several challenges and complexities in the configuration and materials used.

Firstly, there are some essential requirements for the configuration of FZIBs, as summarized in Fig. 2a. (1) Basic configuration: similar to traditional ZIBs, the basic configuration of FZIBs comprises cells assembled with Zn foil anodes and cathodes that include binders, conductive additives, and pure active materials on metal current collectors. During the discharge process, anodic zinc releases electrons and generates Zn^{2+} ions, which are subsequently dissolved by a Zn^{2+}-containing electrolyte. Currently, the Zn^{2+} ions present in the electrolyte traverse the separator and insert into the cathode. The flow of electrons from the anode to the cathode through an external circuit provides the power necessary to operate electrical devices.[42,43] However, the restricted flexibility of zinc metal is inadequate for wearable or flexible applications. Additionally, zinc metal is susceptible to the shape memory effect, preventing it from enduring continuous bending. In order to achieve a truly flexible zinc anode, two common methods have been employed. The first of these involves the application of coating pastes, comprising Zn powders, conductive and binding additives on flexible and conductive current collectors. Another approach is to directly electrodeposit zinc onto flexible substrates. A comparable methodology for the fabrication of flexible cathodes is to deposit active cathode materials upon flexible substrates. This approach is also applicable to the coating of pastes on flexible substrates, which is effective for powder cathode materials. In addition, inspired by the requirement for leak-proof designs, gel electrolytes are favoured for constructing ZIBs in flexible configurations.[44] (2) Flexible device design: the design of the device plays a crucial role in ensuring that the batteries meet the essential requirements for performance and flexibility. Several key aspects of flexible device design include the development of fiber battery design and sandwich structure battery design. Fiber ZIBs exhibit linear shapes and omnidirectional flexibility, which can liberate ZIBs from rigid constraints and bestow upon them greater shape versatilities and design freedoms. The sandwich structure adheres to the conventional principles of battery design. The fabrication of sandwiched ZIBs typically involves numerous steps, including the preparation of flexible electrodes, the sandwiching of the electrolyte and separator between two thin-film electrodes, and subsequent packaging processes.[44,45] (3) Withstand deformation: FZIBs must withstand deformation while maintaining their electrochemical performance. Therefore, the transition from traditional rigid and brittle materials to flexible alternatives is essential for every component of ZIBs.[46–49]

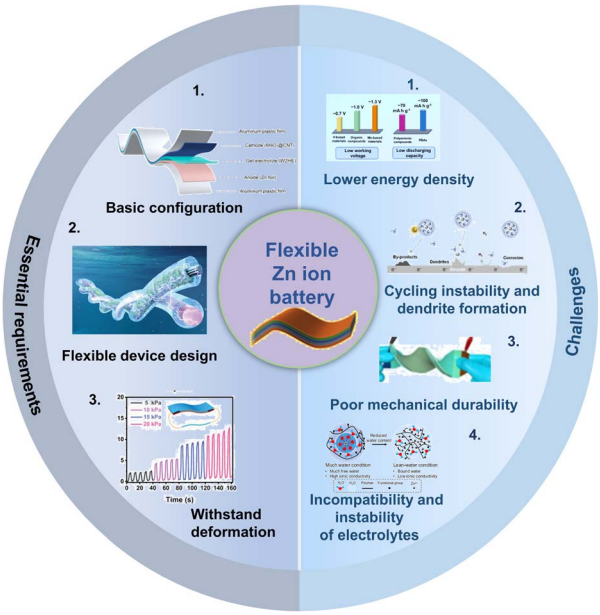

Fig. 2 Essential requirements and challenges of FZIBs. Basic configuration image: reproduced with permission from ref. 50. Copyright 2023, American Chemical Society. Flexible device design image: reproduced with permission from ref. 28. Copyright 2024, Wiley. Withstand deformation image: reproduced with permission from ref. 28 Copyright 2024, Wiley. Lower energy density image: reproduced with permission from ref. 25. Copyright 2022, Wiley. Cycling instability and dendrite formation image: reproduced with permission from ref. 21. Copyright 2023, Wiley. Poor mechanical durability image: reproduced with permission from ref. 43. Copyright 2019, Elsevier. Incompatibility and instability of electrolytes image: reproduced with permission from ref. 24. Copyright 2023, Springer Nature.

Currently, the challenges of FZIBs can be summarized as follows: (1) lower energy density: while ZIBs offer many advantages, their energy density typically lags behind that of LIBs, which is a significant challenge for many applications where both high energy density and flexibility are required. (2) Cycling instability and dendrite formation: repeated charge and discharge cycles can lead to the formation of Zn dendrites. These dendrites can pierce the separator, causing short circuits and battery failure.[50] (3) Poor mechanical durability: the

repeated bending and flexing in applications can strain the mechanical integrity of battery components, leading to potential failures in the electrical connections and separator breakdown.[41,51] (4) Incompatibility and instability of electrolytes: aqueous electrolytes in ZIBs can be prone to water splitting at high voltages, limiting their voltage window and overall performance, while gel electrolytes could expand the voltage range but may introduce other issues of instability or incompatibility.[52]

Addressing these challenges requires innovative approaches in materials science and engineering. For instance, exploring advanced 1D/2D carbon materials for electrodes and separators could enhance the mechanical and electrochemical properties of FZIBs. Additionally, developing novel gel electrolytes with improved stability and compatibility will be crucial for the future success of FZIBs.

2.2. Background of 1D/2D carbon materials

1D/2D carbon materials represent an intriguing and advanced frontier in materials science, due to their distinctive structural, electrical, mechanical, and thermal properties. These materials have gained substantial interest for a broad range of applications including electronics, energy storage, generation, sensors, and composite materials.[53] The following are the background and basic properties of 1D/2D carbon materials:

2.2.1 Carbon nanotubes (CNTs). CNTs were identified by Iijima in 1991 and have since garnered significant attention for exhibiting excellent mechanical properties.[54] CNTs were rolled sheets of graphene in the form of tubes or cylinders and can be divided into two main types: (1) single-walled carbon nanotubes (SWCNTs) which consist of a single layer of graphene rolled into a cylindrical tube and (2) multi-walled carbon nanotubes (MWCNTs) which comprise multiple concentric nanotubes nested within one another, offering enhanced mechanical properties.[55]

2.2.2 Graphene. Graphene consists of planar monolayers of carbon atoms arranged uniformly and tightly in a 2D honeycomb grid structure. This configuration serves as the foundational building block for various graphite materials across different dimensions. It was isolated and characterized in 2004 by Andre Geim and Konstantin Novoselov at the University of Manchester, which earned them the Nobel Prize in Physics in 2010.[56] Graphene also includes graphene oxide (GO) and reduced graphene oxide (RGO). GO is an oxidized form of graphene that is easier to process since it is dispersible in water and other solvents due to the presence of oxygen functionalities. RGO is derived from graphene oxide by removing oxygen-containing groups, partially restoring the conductivity and other properties of pristine graphene.[57]

2.2.3 MXenes. MXenes are a class of 2D materials that are derived from their 3D layered bulk precursors called MAX phases.[58] These MAX phases are ternary carbides, nitrides, or carbonitrides, represented by the formula $M_{n+1}AX_n$, where M represents an early transition metal, A is an A-group element, X is carbon or nitrogen, and n can be 1, 2, or 3.[59,60]

2.2.4 Carbon fibers (CFs). The development of carbon fibers can be traced back to the late 19th century, but significant advancements were made in the 1950s and 1960s. In 1958, Dr Roger Bacon created high-performance carbon fibers at the Union Carbide Parma Technical Center, Cleveland, Ohio. He produced them by heating strands of rayon until they carbonized. This process was later refined using polyacrylonitrile (PAN) as a precursor, which became the most common method for producing CFs.[61]

2.3. Advantages of 1D/2D carbon materials in FZIBs

To address the mentioned challenges of FZIBs, the rational design and construction of carbon-based hybrid electrodes is considered as an effective approach benefiting from multiple exceptional properties of 1D/2D carbon materials. These materials offer numerous advantages (Fig. 3a):

2.3.1 Flexibility and mechanical strength. 1D/2D carbon materials possess exceptional mechanical properties, including outstanding flexibility and tensile strength. This makes them perfect for using in FZIBs which need to maintain performance under mechanical stress such as bending, twisting, and stretching. Furthermore, the high tensile strength of 1D/2D carbon materials contributes to their durability and longevity in FZIBs. They can maintain their mechanical properties even under harsh conditions, providing stable operation and extending the lifespan of FZIBs.[62] In contrast, 0D materials, such as carbon quantum dots, and some 3D carbon materials may lack the necessary flexibility to accommodate mechanical stress, potentially leading to performance degradation or even failure in flexible battery applications.[63]

2.3.2 High specific surface area. 1D/2D carbon materials typically have high specific surface area. This characteristic is crucial for electrodes in batteries as it provides more active sites for ion adsorption and desorption, which can enhance the capacity and rate performance of the batteries. Although 0D carbon materials can offer higher surface area and abundant active sites compared to 1D/2D carbon materials, these active sites are concentrated within individual nanoparticles or molecules, which makes it challenging to achieve uniform distribution throughout the entire material volume. This limitation restricts their efficiency and stability in electrochemical reactions. While 3D carbon materials can provide a certain surface area, it is not as easily conducive to efficient electrochemical reactions as 1D and 2D carbon materials. This may limit their potential applications in high energy density and high rate performance scenarios.[64]

2.3.3 Superior conductivity. 1D/2D carbon materials exhibit excellent electrical conductivity, which helps in achieving lower internal resistance and faster electron mobility within the battery. The high conductivity of these materials ensures efficient charge transfer across the electrode–electrolyte interface, minimizing energy losses and enhancing the overall efficiency of the battery. Moreover, 1D and 2D carbon materials can form efficient conductive networks, enhancing electron transport, which is crucial for maintaining high electrode conductivity and ensuring effective charge–discharge cycles.[65]

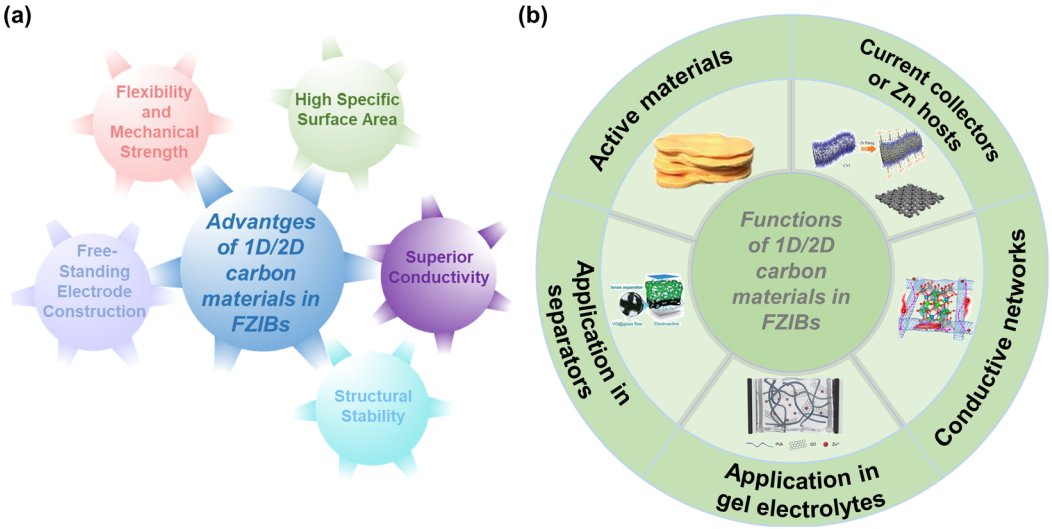

Fig. 3 An overview of (a) the advantages and (b) functions of 1D/2D carbon materials in FZIBs. Active materials image: reproduced with permission from ref. 29. Copyright 2020, Wiley. Conductive networks image: reproduced with permission from ref. 34. Copyright 2022, Elsevier. Current collectors or Zn hosts image: reproduced with permission from ref. 33. Copyright 2019, Wiley. Application in gel electrolytes image: reproduced with permission from ref. 31. Copyright 2021, AAAS. Application in separators image: reproduced with permission from ref. 30. Copyright 2020, Wiley.

In contrast, 0D carbon materials are typically composed of individual nanoparticles or molecules, which have shorter and localized electron and ion transport paths. The lack of continuity between carbon nanoparticles hinders the formation of continuous conductive networks. Therefore, this limitation restricts their performance at high charge–discharge rates. In 3D materials, electrons and ions must traverse longer paths within 3D structures, resulting in higher internal resistance and charge transfer impedance, which ultimately impacts battery performance and efficiency[66]

2.3.4 Structural stability. The robust crystalline structure of 1D/2D carbon materials like graphene helps in preserving the structural integrity of the electrode during the repeated zinc plating and stripping processes that occur during battery charging and discharging.[67] This stability contrasts with that of 0D materials, which are composed of individual nanoparticles or molecules that tend to aggregate or disaggregate easily during electrochemical cycling, leading to structural changes. This phenomenon can significantly impact the long-term stability and cycling life of batteries. Additionally, 3D carbon materials, characterized by their complex 3D structure, experience structural changes and concentration of mechanical stress during extended charge–discharge cycles, contributing to electrode material degradation and performance decline. These factors ultimately limit the stability and reliability of 3D carbon materials over prolonged usage periods.[68]

2.3.5 Free-standing electrode construction. 1D and 2D carbon materials can be fabricated into free-standing electrodes without the need for binders or additional support structures. This reduces the overall weight of the battery and simplifies the manufacturing process, while maintaining structural integrity and electrochemical performance. In contrast, 0D and 3D carbon materials typically lack the inherent structural integrity to be used as free-standing electrodes without a matrix or binder. Their reliance on additional support compromises the overall weight reduction and adds complexity to the manufacturing process. This difference underscores the superior mechanical flexibility and electrochemical performance of 1D and 2D carbon materials in free-standing electrode applications.

Due to the above advantages, 1D/2D carbon materials are excellent candidates for various components in FZIBs, which could be utilized as active materials, conductive networks, current collectors or Zn hosts in FZIBs. Especially, 1D/2D carbon materials are also widely applied in modified separators and gel electrolytes in FZIBs (Fig. 3b). Table 1 summarizes the functions of 1D/2D carbon materials in FZIBs. The details of the functions of 1D/2D carbon materials in FZIBs will be stated in the following text.

3. 1D/2D carbon materials for active materials

1D/2D carbon materials could provide numerous extraordinary properties, which contribute to them being attractive candidates as active materials for FZIBs. Firstly, 1D/2D carbon materials have a high specific surface area (SSA) and abundant pore structure, which can provide more embedded zinc sites, with a higher embedded zinc capacity. Secondly, 1D/2D carbon materials with excellent ionic conductivity facilitate fast ionic transport and reaction kinetics to improve the charge/discharge rate performance of batteries.[42] Additionally, 1D/2D carbon materials also possess reliable chemical and cycling stability, which can reduce the capacity degradation and cycling life loss of the batteries. There have been several studies focusing on the application of 1D/2D carbon materials as active materials for

Table 1 A summary of the functions of 1D/2D carbon materials in FZIBs

Function	Cathode	Anode	Electrolyte	Current density	Cycling number	Capacity retention (%)	Flexibility	Ref.
Active materials	$ZnMn_2O_4$	NHVO@$Ti_3C_2T_x$	3 m Zn $(CF_3SO_3)_2$	2 A g^{-1}	6000	92.1	Folded	69
	V_2CT_X MXene	Flexible Zn	PAMHS	0.5 A g^{-1}	120		Twisted	70
Conductive networks	α-MnO_2@CNT	Zn@CNT	2 M $ZnSO_4$/0.2 $MnSO_4$/PVA	32.5C	1000	100	Bent	71
	ZMO/CNT	Zn foil	1.0 M $ZnSO_4$/0.1 M $MnSO_4$	3 A g^{-1}	2000	97.01	Bent and twisted	34
	CaVO/CNTs	Zn foil	3 M Zn $(CF_3SO_3)_2$	10 A g^{-1}	3000	90.7	Bent	72
	CVO/RCNTs	Zn foil	2 M Zn $(CF_3SO_3)_2$/PVA	5 A g^{-1}	1400	61.5	Bent	73
	KVO/SWCNT	Zn foil	4 M Zn $(CF_3SO_3)_2$	5 A g^{-1}	10 000	91	Bent	74
	MnO_2/CNT/PAA	Zn foil	2 M $ZnSO_4$/0.1 M $MnSO_4$	1.5 A g^{-1}	1000	82	Bent	75
	PDA/CNT/MnO_2	Zn foil	3.3 M $ZnSO_4$	0.2 A g^{-1}	500		Bent	76
	MnO_2	Zn power/CNTs	2 M $ZnSO_4$/0.1 M $MnSO_4$	3 A g^{-1}	2000	91.1	Bent	77
	CNT/MnO_2	ZCN	2 M $ZnSO_4$ + 0.2 M $MnSO_4$	3 A g^{-1}	1000	75.3	Bent	78
	MnO_2/rGO	Zn foil	2 M $ZnSO_4$/0.1 M $MnSO_4$	6 A g^{-1}	500	79	Bent	79
	MnO_2/rGO	Zn foil	2 M $ZnSO_4$/0.1 M $MnSO_4$	2 A g^{-1}	2000	99.87	Bent and folded	80
	RGO/NVO	Zn foil	1 M$ZnSO_4$/1 M $Na2SO_4$	1 A g^{-1}	2000	94	Bent	81
	MnO_2/EG	Zn/EG	2 M $ZnSO_4$/0.1 M $MnSO_4$	1C	480		Bent	82
	$Ti_3C_2T_x$@MnO_2 micro flowers	Zn foil	2.0 M $ZnSO_4$/0.1 M $MnSO_4$	0.5 A g^{-1}	2000	90.6	Bent	83
	CC@MnO_2@MXene	Zn foil	PVA/$ZnSO_4$/$MnSO_4$	1 A g^{-1}	800	51.4	Bent	84
	VO_2/MXene	Zn foil	PVA/Zn $(CF_3SO_3)_2$	5 A g^{-1}	2500	72.1	Bent	85
	ZMO@$Ti_3C_2T_x$	Zn foil	Gelatin-based	1 A g^{-1}	5000	92.4	Flat, bent, and twisted	86
Current collectors or Zn hosts	Co_3O_4 NSs@CNTF	Zn NSs@CNTF	2 M $ZnSO_4$/0.0005 M $CoSO_4$	5 A g^{-1}	10 000	97.27	Bent and twisted	87
	CNT/MnO_2 foams	Zn foil	2 M $ZnSO_4$/0.005 M $MnSO_4$	10 mA cm^{-2}	2500	83.5	Folded	88
	MnO_2@CNT	Zn wire	2 M ZnTFSI/0.2 M $MnCl_2$/PVA	2 A g^{-1}	100	98	Bent and twisted	89
	CNT–MnO_2@PEDOT	Zn/CNT	PVA/LiCl/$ZnCl_2$/$MnSO_4$	20 mA cm^{-2}	1000	88.7	Bent and twisted	33
	FSM@FGF	Zn foil	2 M $ZnSO_4$	1 A g^{-1}	300	82.7	Folded	90
	ZOV array	Zn array	Fumed silica/$ZnSO_4$	20C	2000	89	Bent and twisted	91
	MnO_2@N-VG@CC	Zn@N-VG@CC	PVA/Zn $(CF_3SO_3)_2$	2 A g^{-1}	300	80	Bent and twisted	92
	PANI/SWCNTs	Zn/RGO–SWCNTs	PVA/Zn $(CF_3SO_3)_2$	1 A g^{-1}	1000	97.3	Flat, bent, and twisted	93
	N-CNSs@MnO_2	N-CNSs@Zn	PVA	8 A g^{-1}	500	76.5	Bent and twisted	94
	Al_2O_3@VSe_2NSs@N-CNFs	Zn NSs@CNT	CMC/$ZnSO_4$	1 A g^{-1}	2500	86.2	Bent	95
	V_2O_5-CFC	Zn foil	2 M $ZnSO_4$/0.1 M $MnSO_4$	0.5 A g^{-1}	1000		Bent	96
	V_2O_3@CNFs	Zn@CC	2 M Zn $(CF_3SO_3)_2$	2 A g^{-1}	1000		Bent and twisted	97
	MnO_2@CC	Zn foil	PAM/$ZnSO_4$/$MnSO_4$	0.1 A g^{-1}	300		Bent	98
	MnO_2	CC@MnO_2-UTF@Zn	2 M $ZnSO_4$/0.2 M $MnSO_4$	1 A g^{-1}	300	81	Flat and bent	99
	VS_2/CC	Zn/CC	PVA/Zn $(CH_3COO)_2$/Mn $(CH_3COO)_2$·				Flat, bent, and twisted	100
Application in gel electrolytes	MnO_2	Zn foam	PVA/GO	0.3 A^{-1}	1000	98	Flat, bent, and twisted	31
	V_2O_5	Zn foil	V_2O_5/GO/PVA	1 A g^{-1}	1000	96	Bent and twisted	101
	V_2O_5	Zn foil	PVA/Zn $(CF_3SO_3)_2$/TiO_2	0.2 A g^{-1}	100	99.8	Flat and bent	102
Application in separators	V_2O_5	Zn foil	2 M $ZnSO_4$	5 A g^{-1}	1000	75	Flat and bent	30
	V_2O_5	Zn foil	2 M Zn $(CF_3SO_3)_2$	1 A g^{-1}	1000	78.7	Bent	103

FZIBs. For example, 1D/2D carbon materials such as MXenes, which have been adopted as active materials for FZIBs. These studies have proved that 1D/2D carbon materials could exhibit well-embedded zinc properties, high specific capacity and excellent cycling stability in FZIBs.

Modeled on the method of inhibiting dendrite growth in a lithium-ion battery system, the construction of rocking-chair type zinc-free metal anode materials will be an effective way to solve the growth of zinc dendrites.[14] MXene is a class of 2D layered transition metal carbides or nitrides, with interlayer spaces capable of accommodating and storing zinc ions, which makes it an ideal zinc ion storage material. As active materials for zinc storage, MXenes offer high capacity, rapid ion transport, and excellent mechanical properties, among other advantages. Yuan *et al.* synthesized $(NH_4)_2V_{10}O_{25}\cdot 8H_2O$@$Ti_3C_2T_x$ (NHVO@$Ti_3C_2T_x$) films by vacuum filtration of 1D ultrathin NHVO nanobelts and layered $Ti_3C_2T_x$ nanosheets. The composite film exhibited a low working potential of 0.59 V and could be utilized as an anode for "rocking-chair" type ZIBs. More importantly, 2D $Ti_3C_2T_x$ not only provided a flexible substrate for NHVO, which could be bent and folded, with an excellent mechanical performance, but also stabilized the structural changes of NHVO nanobelts during charge and discharge. In the meantime, the utilization of MXenes as active materials yielded a specific capacity. Consequently, the NHVO@$Ti_3C_2T_x$ thin film electrode delivered a remarkable capacity of 514.7 mA h g^{-1} over 6000 cycles, retaining a capacity of up to 84.2%. The "rocking-chair" Zn-ion full battery constructed by pairing the NHVO@$Ti_3C_2T_x$ thin film anode and the $ZnMn_2O_4$ cathode exhibited a maximum specific capacity of 131.7 mA h g^{-1} and a maximum energy density of 97.1 W h kg^{-1}, which is better than those of the previously reported "rocking-chair" Zn-ion battery.[69] In addition, Li.*et al.* presented an aqueous zinc hybrid-ion battery (ZHIB) featuring a remarkable capacity enhancement over 18 000 cycles, utilizing a 2D layered V_2CT_X MXene cathode. Here, "T_X" denoted the surface functional groups such as –F, –OH, and = O, which significantly differed from those in previously reported ZHIBs. The delamination of V_2CT_X MXene enabled a continuous exposure of active sites, and the phase transition product in conjunction with V_2CT_X MXene contributed continuously to capacity, which accounted for the unusual capacity enhancement.[70]

While MXenes are promising in these diverse applications, several challenges need addressing to fully exploit their potential: (1) MXenes are susceptible to oxidation, which can degrade their properties. Enhancing their stability under environmental conditions is crucial for practical applications. (2) Methods for the synthesis and processing of MXenes need improvement to ensure that they can be produced in large quantities without losing quality. (3) Concerns regarding the toxicity of MXenes and their precursors, particularly those involving hazardous chemicals like hydrofluoric acid, need to be addressed. Developing safer synthesis methods and handling protocols is essential. Addressing these challenges will be key to advancing the use of MXenes as active materials across various domains. With ongoing research and development, MXenes hold the potential to revolutionize multiple industries by providing high-performance alternatives to traditional materials.

4. 1D/2D carbon materials for conductive networks

The combination of 1D/2D carbon materials with superior electrical conductivity and electrode materials can significantly enhance the conductivity and flexibility of electrodes, thereby improving their zinc storage performance. For details, 1D carbon materials, such as carbon nanotubes, exhibit elongated and thin structures resembling rolled-up single-layer carbon atoms, facilitating the formation of continuous conductive pathways. 2D carbon materials, like graphene, consist of a single-layer planar lattice of carbon atoms with a smooth and extensive surface area, promoting efficient electron transport and conductivity. These structural features enable electrons to move freely along extended 1D or 2D structures, creating longer electron transport paths and ultimately forming superior conductive networks.[42]

4.1. Carbon nanotubes as conductive networks

4.1.1 Carbon nanotubes as conductive networks for cathodes. As 1D carbon materials, CNTs exhibit tensile strength up to 63 GPa and electrical conductivity up to 5×10^5 S m^{-1}, and could withstand high current density (4×109 a cm^{-2}).[104] These properties provide CNTs with excellent electrical conductivity and flexibility, which enable them as conductive substrates to support active materials. Impressively, Bi and colleagues pioneered the fabrication of CNT foams through chemical vapor deposition (CVD), followed by the uniform electrodeposition of amorphous MnO_2 (a-MnO_2) onto the CNT foam-based scaffolds (α-MnO_2@CNTs). This electrodeposition process occurred in a solution containing 1 M $KMnO_4$ and 0.1 M H_2SO_4 at 50 °C. After acid treatment, hydrophilic CNTs served as a template for the reduction of $KMnO_4$ and as a conductive substrate to support the uniform dispersion of α-MnO_2 nanosheets. The synergistic effect of the highly disordered porous CNT network and amorphous manganese dioxide provided more active sites, accelerating ion diffusion and reaction kinetics. Hybrid electrodes based on α-MnO_2@CNTs exhibited high energy density and stable cycling performance (Fig. 4a and b). More importantly, the prepared electrodes exhibited outstanding mechanical performance. Flexible quasi-solid rechargeable ZIBs were fabricated with α-MnO_2@CNT as the cathode and electrodeposited Zn@CNT as the anode (Fig. 4c), which showed stable electrochemical performance under various bending conditions.[71] The intrinsic high electrical conductivity of CNTs significantly reduces the overall resistance of the cathode material. This is of paramount importance for the efficient transfer of electrons during the charge and discharge cycles.

Furthermore, CNTs provide mechanical strength to the cathode structure. Their high tensile strength and flexibility contribute to maintaining the integrity of the electrode even under mechanical stress, which is particularly important for flexible or wearable applications. As depicted in Fig. 4d, Gao

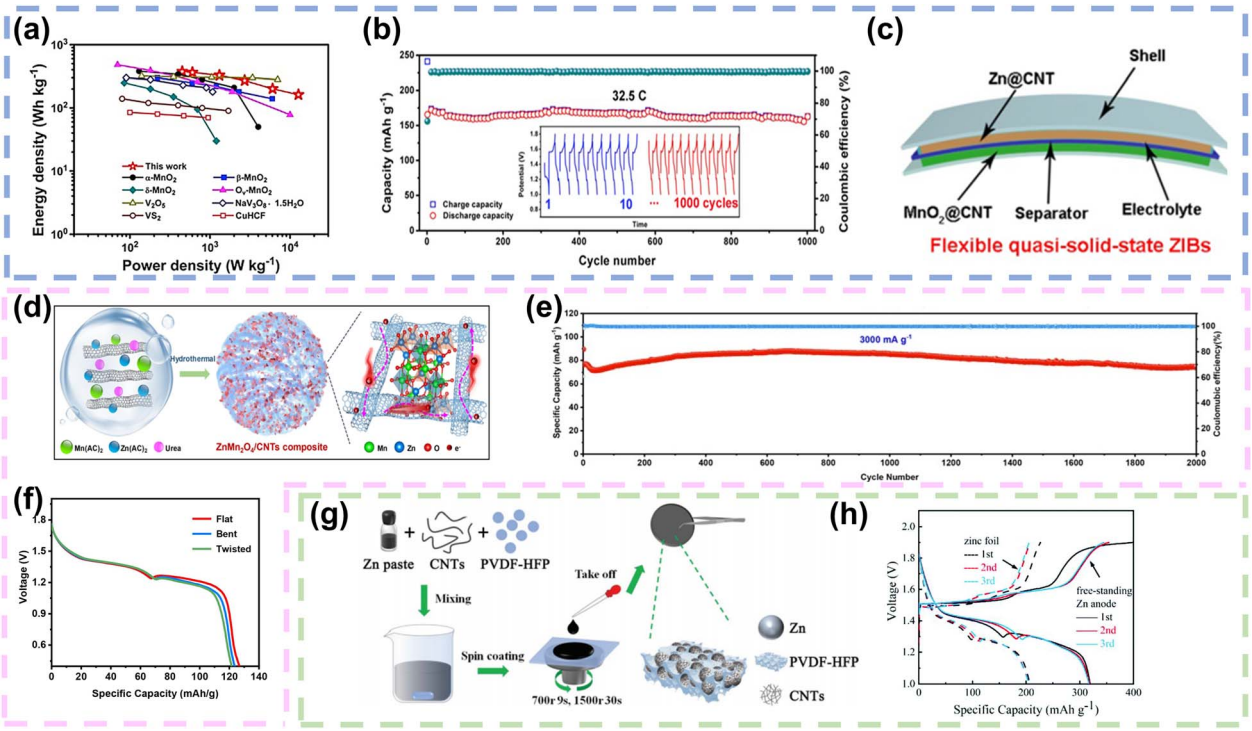

Fig. 4 Carbon nanotubes as conductive networks in FZIBs. (a) Ragone plot illustrating the energy and power densities in comparison with that of other previously reported cathode materials in aqueous ZIBs. (b) The cycling performance and galvanostatic charge/discharge curve of α-MnO_2@CNTs at 32.5C. (c) The fabricated flexible quasi-solid-state ZIBs. Reproduced with permission from ref. 71. Copyright 2020, Elsevier. (d) Scheme illustrating the fabrication of ZMO/CNTs. (e) Cycling performance of the ZMO/CNT electrode at 3000 mA g^{-1}. (f) Discharging curves at 100 mA g^{-1} under different conditions of FZIBs. Reproduced with permission from ref. 34. Copyright 2022, Elsevier. (g) The fabrication process of the free-standing Zn anode. (h) Discharge/charge curves of ZIBs with the freestanding Zn anode and zinc foil at 0.3 A g^{-1}. Reproduced with permission from ref. 77. Copyright 2021, the Royal Society of Chemistry.

et al. synthesized ZMO/CNT cathodes by anchoring $ZnMn_2O_4$ particles onto CNTs through a one-step hydrothermal method. Due to robust interfacial interactions (Mn–O–C bond) enhanced both the electron and ion transport pathways, the ZMO/CNT cathode demonstrated high capacity and remarkable cycling life, with a capacity retention of 97.01% even after 2000 cycles (Fig. 4e). In addition, the FZIB was assembled with the ZMO/CNT as the cathode and zinc foil as the anode, which was enough for it to be bent or twisted and the electrochemical impedance in the bent or twisted states was similar to that in the flat state (Fig. 4f).[34] Parallelly, CaVO microflowers were successfully synthesized using a hydrothermal method. Subsequently, CaVO/CNT films were effectively prepared using spray printing technology. The CaVO microflowers were enveloped by a network of CNTs, expediting electron transport and enhancing electrical conductivity. Furthermore, the fabricated CaVO/CNT film demonstrated remarkable flexibility, and its electrochemical performance remained stable under different bending conditions.[72]

4.1.2 Carbon nanotubes as conductive networks for anodes. Impressively, CNTs can also serve as conductive networks in Zn anodes, enhancing their electrochemical performance and stability. The unique structural properties of CNTs facilitate efficient electron transport and ion diffusion within the Zn electrode. For example, lightweight and flexible CNT frameworks with large SSA profiles were assembled with nano/microstructure Zn powders and film-formers to construct flexible zinc thin film electrodes, which replaced conventional Zn foil electrodes. Gao and colleagues synthesized a free-standing thin Zn powder film as the anode by homogeneously dispersing Zn podwer and CNTs in the poly vinylidene fluoride hexafluoropropylene (PVDF-HFP) binder, adopting the spin-coating process (Fig. 4g). For the Zn anode, the high mechanical properties were attributed to the three-dimensional interconnection network, which was formed by the well-dispersed CNTs and PVDF-HFP. Overall, CNTs mainly improved the electrical conductivity, while the presence of PVDF-HFP was crucial for film formation and excellent flexibility. At an optimum Zn powders/CNTs/PVDF-HFP ratio of 80 : 12 : 8, the freestanding zinc thin film electrode exhibited a specific capacity of 318.5 mA h g^{-1} at a current density of 0.3 A g^{-1} (Fig. 4h).[77] In a similar manner, nanocellulose was employed as a film-forming agent, and dispersed Zn microspheres along with CNTs were assembled into free-standing ZCN thin film electrodes through a straightforward vacuum filtration process. In this study, Zn powders structured with microspheres of several μm in diameter provided numerous advantages as active materials. Among these, including plentiful electroactive sites and 3D diffusion pathways contributed to the reversible plating/

stripping of Zn^{2+} ions and ultimately enhanced the cycling life and performance stability of ZIBs.[78]

By introducing CNTs with various nanostructures and excellent properties, the issues associated with cathodes and anodes in FZIBs can be effectively addressed. When conductive CNTs are combined with low conductivity cathode materials, the resulting hybrid electrodes are expected to exhibit excellent zinc storage performance.[42] While CNTs offer significant advantages as conductive networks in both cathodes and anodes of FZIBs, their integration into battery systems also presents challenges. (1) Dispersion and homogeneity: achieving a uniform dispersion of CNTs within electrode materials is challenging due to their tendency to agglomerate. Proper dispersion techniques are essential to ensure that CNTs are evenly distributed, maximizing their beneficial effects on conductivity and mechanical properties. (2) Cost and scalability: the production of CNTs can be costly, and scaling these processes while maintaining quality and performance poses significant challenges. Reducing the cost of CNT production is crucial for their widespread adoption in commercial FZIB applications.

CNTs offer several compelling advantages for both cathodes and anodes in FZIBs, enhancing ionic conductivity, structural integrity and mechanical durability. However, addressing challenges related to dispersion, cost, and material compatibility is crucial for realizing the full potential of CNTs in this promising area of energy storage technology. Ongoing research and development are expected to continue improving the integration of CNTs in FZIBs, paving the way for more reliable, safe, and efficient flexible batteries.

4.2. Graphene as a conductive network

Owing to the advantages of high intrinsic strength, great transmittance, superior thermal conductivity and high electron mobility, graphene is considered as an advantageous conductive network for enhancing the electrical conductivity of FZIBs. The exceptional electrical conductivity facilitates rapid and efficient electron movement, which is critical for high-performance batteries. Its superior thermal conductivity helps manage heat dissipation, enhancing the safety and longevity of devices. Additionally, the high intrinsic strength of graphene contributes to the mechanical stability of the conductive network, ensuring durability during repeated charge–discharge cycles. Additionally, graphene nanosheets can be assembled with active materials into conductive and flexible composite films, preventing the self-stacking of graphene nanosheets and the agglomeration of active materials. Most importantly, graphene nanosheets can be easily assembled into 1D fibres and 2D films. What's more, its high electrical conductivity enables rapid and efficient charge transport within the FZIBs, thereby reducing internal resistance and enhancing the power density

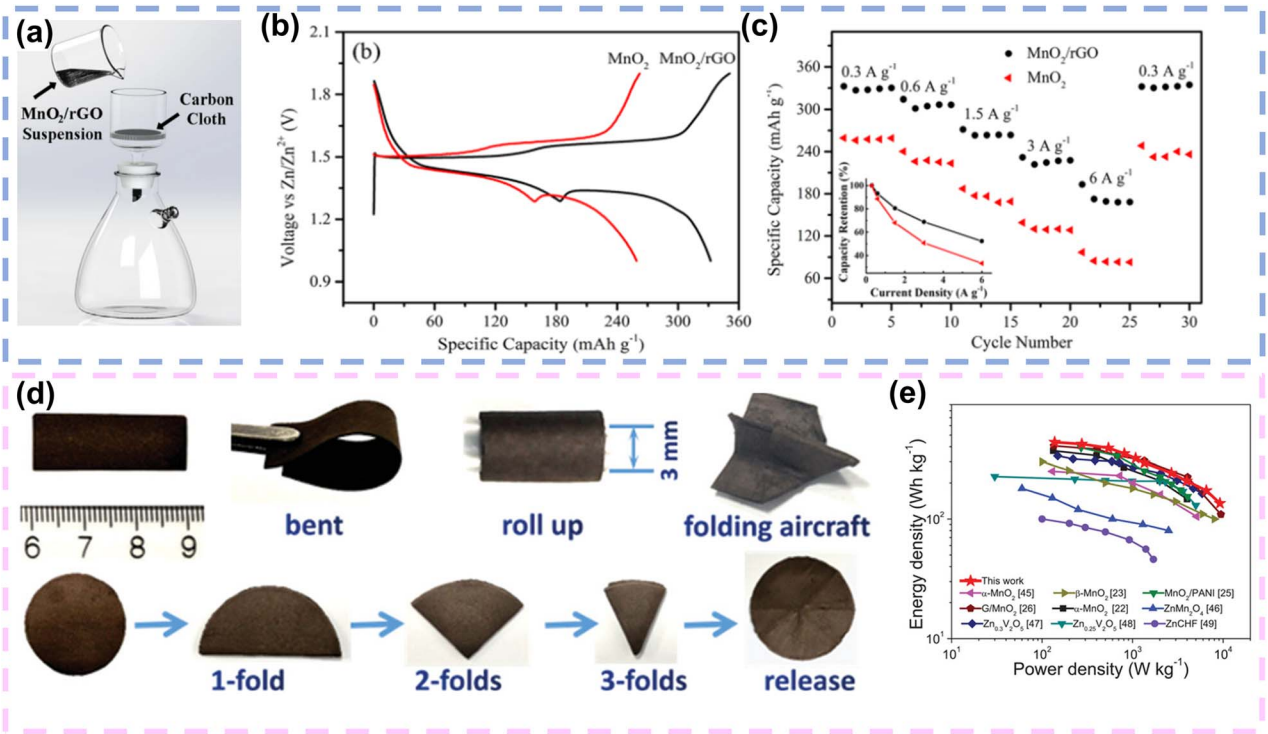

Fig. 5 Graphene as a conductive network in FZIBs. (a) Schematic illustration of the vacuum filtration on carbon cloth to prepare MnO_2/rGO electrodes. (b) Comparison of the charging and discharging profiles of the samples at a current density of 0.3 A g^{-1}. (c) Specific capacities (normalized over the mass of MnO_2) of the samples at different current densities. Reproduced with permission from ref. 79. Copyright 2018, Springer nature. (d) The digital photos of the MnO_2/rGO nanocomposite membrane demonstrating flexibility under bent, rolled, and folded conditions. (e) Ragone plot of our cells compared with previously reported ZIBs. Reproduced with permission from ref. 80. Copyright 2020, Wiley.

of FZIBs.[105] For example, Huang and colleagues deposited MnO_2 nanosheets and reduced graphene oxide (rGO) sheets onto carbon cloth to fabricate a binder-free MnO_2/rGO hybrid cathode by vacuum filtration (Fig. 5a). Due to the uniform deposition of MnO_2/rGO on carbon cloth without a binder, the electrode's internal resistance was reduced. Consequently, in comparison to the traditional MnO_2 cathode, the hybrid cathode exhibited higher capacity (Fig. 5b), excellent rate performance (Fig. 5c), and stable cycling performance. When the Zn//MnO_2/rGO battery was assembled, the highly flexible battery maintained a capacity retention rate of 90% after 500 cycles under conditions of bending at an angle close to 180°.[79] More importantly, the nanostructures are currently a research hotspot for further realizing high-energy/power density, long life, light weight, and superior mechanical properties under various deformation conditions. In 2018, Wang *et al.* constructed MnO_2/rGO lightweight thin film electrodes, which employed 1D ultralong MnO_2 nanowires with a high aspect ratio and 2D rGO nanosheets. The unique 1D/2D structure enabled the thin film electrode to have excellent mechanical deformation performance, and it could be folded into shapes such as paper airplanes (Fig. 5d). Impressively, the free-standing hybrid nanoarchitecture could reduce the transfer path of electrons, which allowed the electrode to exhibit an energy/power density of 436 W h kg^{-1}/9.2 kW kg^{-1}(Fig. 5e).[80]

Similarly, Wan and colleagues fabricated free-standing RGO/NVO films using high aspect ratio NVO nanobelts and RGO through vacuum filtration. Benefiting from the multilayer connection between the RGO sheet and the NVO nanobelt, the RGO/NVO hybrid film not only exhibited excellent mechanical performance, but also much improved electrical conductivity. The manufactured flexible soft-packaged ZIBs were able to operate stably under different conditions and showed no significant capacity decay after 100 cycles.[81] Significantly, Dong's group generated transparent graphene nanosheets with a thickness of 14 μm, which were prepared by simple electrochemical exfoliation. The flexible hybrid films were prepared by vacuum filtration of electrochemically exfoliated graphene (EG) nanosheets and ultrathin MnO_2 nanosheets. The availability of EG provided free-standing MnO_2/EG films with superior flexibility. In addition, the highly flexible EG nanosheets could also serve as a conductive substrate for electrodepositing Zn, which was obtained as a Zn/EG film electrode instead of rigid Zn foil. Owing to the significant effect of EG on slowing down the dissolution of Mn and regulating the volume change during charge/discharge cycles, the MnO_2/EG//Zn/EG full battery assembled with MnO_2/EG as the cathode and Zn/EG as the anode exhibited a high specific capacity of 300 mA h g^{-1} at 0.2C. A critical feature of the soft-packaged MnO_2/EG//Zn/EG battery was its outstanding flexibility, allowing the battery to maintain the brightness of a small bulb even when bent and deformed. This further validated the importance of EG nanosheets in flexible and high-performance ZIBs.[82]

In particular, mass loading refers to the amount of active material per unit area in the cathode, which directly influences the energy density and overall performance of batteries. According to recent studies, He's team successfully synthesized a sodium and copper co-intercalated boron titanate manganese oxide (NCMO) cathode. When using TIMCAL graphite & carbon as a conductive material, it exhibited highly reversible Mn deposition and dissolution processes under high-quality loading, attributed not only to the dual-ion co-intercalation increasing the manganese conversion on the cathode surface but also to the stability of the host material during charge/discharge cycles.[106] Moreover, in high-loading cathode ZIBs, the use of 1D/2D carbon materials can create a conductive network that improves electron transport pathways and mechanical stability. This network allows for a higher amount of active material to be effectively utilized, thereby increasing the overall capacity and energy density of FZIBs. The high specific surface area and excellent electrical conductivity of these 1D/2D carbon materials facilitate the uniform distribution and robust connection of active materials, thus supporting higher mass loadings without compromising the battery's performance. This network allows for a higher amount of active material to be effectively utilized, thereby increasing the overall capacity and energy density of FZIBs. Furthermore, the structural integrity provided by 1D/2D carbon materials can prevent the detachment of active materials during cycling, enhancing the longevity and cycling stability of FZIBs.

Although graphene offers numerous benefits, its large-scale production remains cost-intensive and technically challenging. Reducing the cost of graphene production through improved synthesis methods is crucial for its broader adoption in commercial applications. Moreover, achieving effective integration of graphene with existing battery materials requires advanced material engineering techniques. What's more, while graphene's general properties are well understood, optimizing these properties for specific battery configurations and applications remains an area of active research. In conclusion, graphene as a conductive network in FZIBs represents a significant advancement in battery technology, particularly for applications requiring high flexibility, durability, and performance. Its ability to enhance both the cathode and anode properties addresses several limitations of traditional battery materials, positioning graphene as a key material in the future advancement of energy storage devices. Continuing advancements in graphene processing and integration will likely unlock further potential of this versatile material in flexible battery applications.

4.3. MXenes as conductive networks

Benefiting from their abundant functional groups, high conductivity, superior electrochemically active surface area, hydrophilicity and excellent mechanical properties, MXenes are considered as an appropriate 2D template or conductive network to accommodate for carrying high capacity active materials.[107,108] First of all, MXenes typically demonstrate high electrical conductivity, often ranging from 10^4 to 10^5 S m^{-1}. This high conductivity facilitates efficient electron transport, reducing internal resistance in batteries and improving their power density. Secondly, MXenes possess a large SSA, and this high SSA enhances electrode–electrolyte contact, promoting ion

transport and electrochemical reactions, thereby enhancing battery performance. What's more, MXenes demonstrate good chemical stability, maintaining robust performance in various electrochemical environments. For instance, Shi *et al.* synthesized 3D $Ti_3C_2T_x$@MnO_2 microflower electrodes with a gas-phase spray drying approach. The etching $Ti_3C_2T_x$ nanosheets were uniformly dispersed in Mn $(NO_3)_2$ salt solvent to form a mixed solution, which was introduced into a spray atomizer to generate aerosol droplets. These droplets were subsequently transferred into a high-temperature reactor under the action of a carrier gas. Benefiting from the solvent evaporation and capillary forces generated by the $Ti_3C_2T_x$ nanosheets in the high temperature reactor, 3D $Ti_3C_2T_x$@MnO_2 microflower structures were successfully constructed (Fig. 6a). The $Ti_3C_2T_x$ nanosheets were encapsulated with MnO_2 nanoparticles. Notably, the (002) characteristic peak of $Ti_3C_2T_x$-Mxene and the typical characteristic peak of γ-MnO_2 were clearly shown in the XRD pattern of 3D $Ti_3C_2T_x$@MnO_2 microflowers, consisting of 1×1 ($\approx 2.3 \times 2.3$ Å, pyrolusite) and 1×2 ($\approx 2.3 \times 4.6$ Å, ramsdellite) randomly oriented tunnels composed of γ-MnO_2, which facilitated Zn^{2+} storage. When employed as a cathode, the 3D $Ti_3C_2T_x$@MnO_2 microflower structure demonstrated commendable reversible capacity and rate performance. Impressively, it showcased a remarkable capacity retention of 90.6% even after undergoing an extensive 2000 cycles. Pairing the 3D $Ti_3C_2T_x$@MnO_2 microflower cathode with a Zn nanosheet anode electrodeposited on carbon cloth, the FZIB was assembled with gel electrolyte (Fig. 6b). Fig. 6c illustrated the impressive power delivery of the FZIB after full charging. A single device was capable of powering both an electric clock and a light-emitting diode (LED). Even during dynamic bending, the FZIB maintained its performance, with the LED indicator continuing to emit a bright red light. Impressively, the FZIB exhibited similar specific capacity and cycling performance under different bending conditions (Fig. 6d).[83] Similarly, Qi *et al.* utilized carbon cloth with remarkable flexibility and conductivity as the substrate. They employed an electrodeposition process to grow MnO_2 nanosheets directly onto its surface. To further improve the conductivity, MXene coating was added on the surface of the MnO_2 nanosheets to synthesize a binder-free CC@MnO_2@MXene electrode. The electrode exhibited excellent electrochemical performance owing to the presence of MXenes, which improved the conductivity of the electrode and facilitated the co-intercalation mechanism of Zn^{2+} and H^+ (Fig. 6e). Fig. 6f displayed the CV curves of the quasi-solid CC@MnO_2@MXene//Zn flexible battery in both normal and bent states. The curves exhibited two reduction peaks at approximately 1.19 and 1.3 V, along with a broad oxidation peak at around 1.7 V, demonstrating that bending did

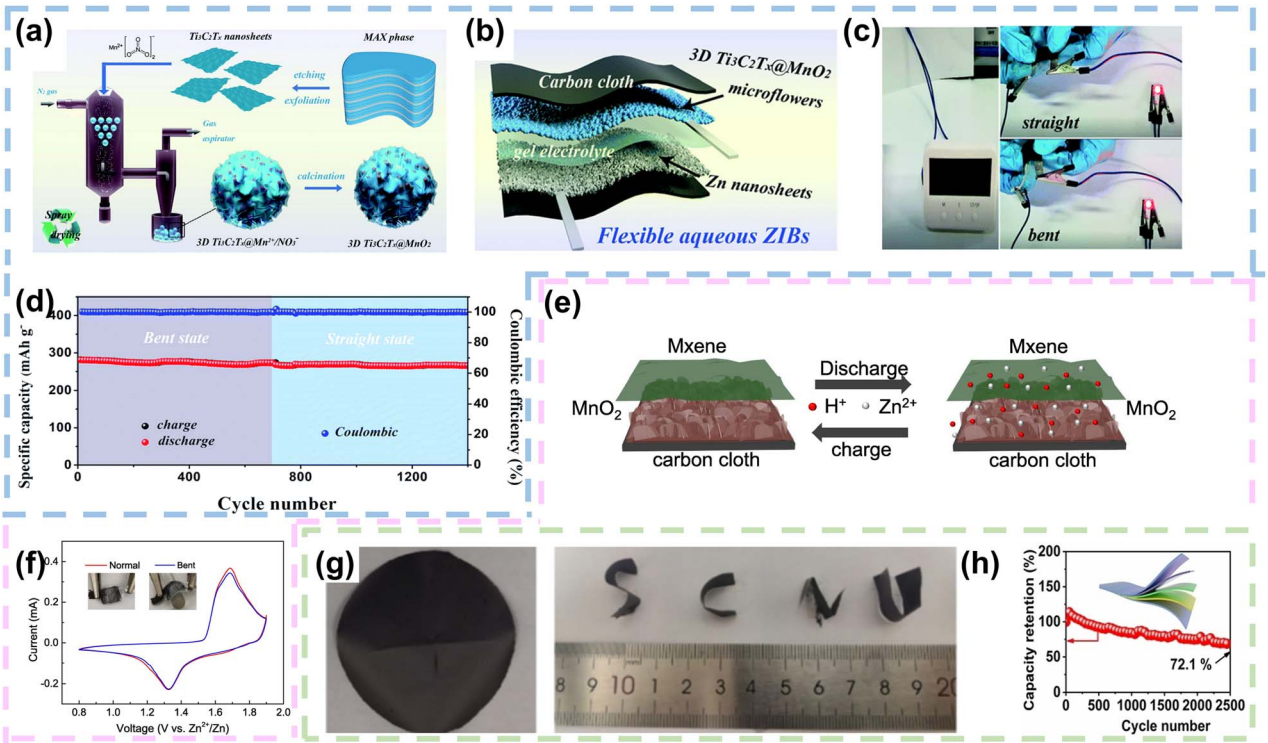

Fig. 6 MXenes as conductive networks in FZIBs. (a) Schematic depiction of the synthesis process of 3D $Ti_3C_2T_x$@MnO_2 microflowers. (b) Fabrication procedure for the FZIB. (c) Real-time image demonstrating the FZIB supplying power under both straight and bent conditions. (d) Cycling performance in the straight and bent states at a current density of 100 mA g^{-1}. Reproduced with permission from ref. 83. Copyright 2020, the Royal Society of Chemistry. (e) Schematic representation of intercalation and deintercalation mechanisms of the CC@MnO_2@MXene electrode. (f) CV curves under normal and bending conditions. Reproduced with permission from ref. 84 Copyright 2022, Elsevier. (g) Optical images of the VO_2/MXene hybrid films. (h) Cycling performance of the VO_2/MXene hybrid films at a current density of 5 A g^{-1}. Reproduced with permission from ref. 85. Copyright 2021, Wiley.

not affect the electrochemical performance of CC@MnO_2@MXene.[84]

Furthermore, considering the inherent excellent conductivity and mechanical properties of 2D MXenes, Shi *et al.* fabricated VO_2/MXene hybrid films through a simple vacuum filtration process. Within the hybrid film, VO_2 nanoparticles were embedded within MXene sheets, establishing a 3D layered conductive network. Optical images revealed that the VO_2/MXene hybrid film exhibited high flexibility and remained free of cracks under various bending and folding states (Fig. 6g). The specific capacity of the VO_2/MXene hybrid film reached up to 228.5 mA h g^{-1}, with an energy density of up to 197.2 W h kg^{-1}. To demonstrate the application of VO_2/MXene hybrid films in flexible energy storage devices, the researchers designed a quasi-solid-state FZIB with the hybrid film as the cathode material. Moreover, the flexible battery exhibited remarkable mechanical flexibility and exceptional Zn^{2+} storage capacity, maintaining a capacity retention of 72.1% after 2500 cycles at 5 A g^{-1}(Fig. 6h).[85] In conclusion, the ability of MXenes to form continuous conductive pathways enhances electron transport efficiency in batteries, leading to improved electrochemical performance. Their high surface area provides ample active sites for electrochemical reactions, increasing the capacity and rate performance of energy storage devices. Additionally, MXenes possess good mechanical flexibility and chemical stability, which are crucial for maintaining the structural integrity and longevity of electrodes during cycling. Furthermore, MXenes can be functionalized to tailor their surface chemistry, allowing for the optimization of their electrochemical properties to meet specific application needs. The combination of these properties positions MXenes as a promising material for advanced conductive networks, contributing to the development of high-performance and durable energy storage systems.

5. 1D/2D carbon materials for current collectors or Zn hosts

Traditional metal current collectors, owing to their high mass, are unsuitable for achieving light weight and flexibility. To address this issue, researchers focused on 1D/2D materials, leveraging their inherent structural advantages to develop lightweight and flexible current collectors. Beyond their role as current collectors, 1D/2D carbon materials also function effectively as Zn hosts for electrochemical deposition of zinc; this approach replaces the use of heavy and rigid zinc foil, which improves energy density and enables high mechanical flexibility of FZIBs.[109,110]

5.1. CNTs as current collectors or Zn hosts

5.1.1 CNTs as current collectors for cathodes. Individual CNTs can be woven into porous networks or thin films to facilitate the loading and rapid electron transfer of active materials, which can serve as current collectors for FZIBs. For instance, Zhao's team developed a flexible fiber-shaped electrode featuring 3D ultrathin Co_3O_4 nanosheets organized on a carbon nanotube fiber (Co_3O_4 NSs@CNTF). This was achieved through a straightforward *in situ* oxidation process applied to a self-assembled Co-based metal–organic framework (MOF) on a carbon nanotube fiber (Co-MOF@CNTF) (Fig. 7a). The fiber-shaped electrode demonstrated high specific capacity, excellent rate performance, and high voltage in a mild, neutral aqueous electrolyte. Furthermore, the cycling stability of the electrode was markedly augmented to 10 000 cycles through the implementation of an electrolyte dynamics engineering strategy, which involved the addition of trace amounts of Co^{2+} cations to a 2 M $ZnSO_4$ aqueous electrolyte to prevent the dissolution of the Co_3O_4 NSs@CNTF cathode (Fig. 7b and c). Moreover, the electrochemical performance of the assembled fiber shaped ZIB remained stable even after 2000 bending cycles at 120 angle, demonstrating remarkable flexibility and durability. Finally, the fiber shaped ZIBs were integrated into a sweater and connected in series to power a smart watch with high safety, indicating significant potential for applications in flexible and wearable electronics.[87] In addition, to accommodate the volume change during the additional MnO_2 redox deposition and dissolution, Li and co-workers electrodeposited MnO_2 nanoflakes on CNT films to obtain a binder-free CNT@MnO_2 film, where MnO_2 nanoflakes were uniformly dispersed on the CNT surface (Fig. 7d), since the 3D porous structure of the CNT could provide a robust scaffold for MnO_2 deposition and dissolution and electrolyte reservation. As shown in Fig. 7e, the pouch-type Zn–MnO_2 battery exhibited good cycling durability with about 83.5% capacity retention after 2500 cycles.[88] Similarly, Ma and colleagues firstly fabricated CNT fibers with diameters of approximately 80–100 μm by using Fe films as catalysts in a chemical vapor deposition (CVD) process, where arrays of CNTs were grown directly on silicon wafers. Subsequently, MnO_2@CNT fiber electrodes were achieved in an aqueous Mn $(NO_3)_2$ solution through a chronoamperometric electrochemical deposition process, resulting in MnO_2 nanosheets densely wound and grew vertically on the surface of the CNT fibers. The Zn//MnO_2 cable-like micro battery assembled with MnO_2@CNT fibers as the cathode, zinc wire as the anode and $ZnCl_2$ gel polymer as the electrolyte achieved a specific capacity of 290 mA h g^{-1} at 0.1 A g^{-1}. In addition, the Zn//MnO_2 cable-like microcell exhibited superior flexibility, which was almost identical to the flat galvanostatic charge/discharge curve after 100 bending cycles.[89]

In a word, while CNTs have shown great potential in the realm of flexible energy storage devices, the development of CNT-based current collectors is still an evolving field with many challenges to overcome. One major obstacle is the inherently low electrical conductivity of individual CNTs when assembled into macroscopic structures, which limits their performance as current collectors. Furthermore, the mechanical properties of CNTs can degrade over long-term cycling or under repeated mechanical deformation, affecting the durability and reliability of the devices. Advancements in material engineering, surface chemistry, and fabrication techniques are essential to fully realize the potential of CNTs in creating high-performance, durable, and flexible energy storage devices. Future research should focus on addressing these challenges to enable the

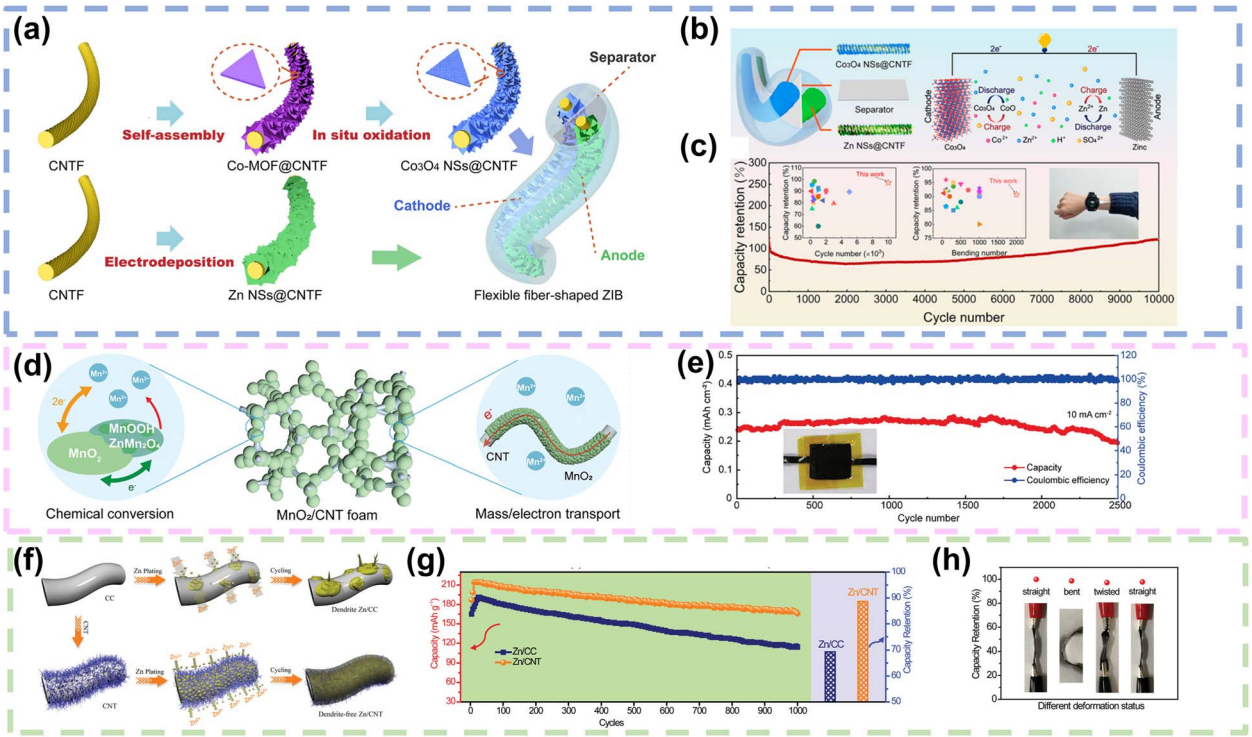

Fig. 7 CNTs as current collectors or Zn hosts in FZIBs. (a) Schematic depiction of the preparation process of fiber shaped Co_3O_4 NSs@CNTF and Zn NSs@CNTF electrodes. (b) Schematic diagram of the mechanism of the aqueous ZIB employing Co_3O_4 NSs@CNTF as the cathode and zinc as the anode. (c) Long-term cycling performance of a fiber-shaped ZIB at a current density of 5 A g^{-1}; comparison of long-term cycling performances for the fiber-shaped ZIB in this work and a previous FZIB and an image of flexible fiber shaped ZIBs integrated into a sweater to charge a smart watch. Reproduced with permission from ref. 87. Copyright 2021, American Chemical Society. (d) Diagram illustrating the MnO_2/CNT foam cathode with a reversible chemical conversion and a 3D hierarchical structure for mass and charge transport. (e) Cycling performance of the assembled Zn–MnO_2 battery that was tested at 10 mA cm^{-2}. Reproduced with permission from ref. 88. Copyright 2021, Wiley. (f) The schematic illustrations of Zn deposition on CC and CNT electrodes. (g) Cycling performance measured at 20 mA cm^{-2} of the Zn//MnO_2 batteries with Zn/CC and Zn/CNT anodes tested in aqueous electrolyte with a coin cell. (h) Capacity retention of the quasi-solid-state Zn//MnO_2 battery with a Zn/CNT anode under different deformation states. Reproduced with permission from ref. 33. Copyright 2019, Wiley.

widespread adoption of CNT-based current collectors in commercial applications.

5.1.2 CNTs as Zn hosts. Hollow multiwalled CNT arrays could be woven into a 3D conductive and porous CNT network on a carbon cloth (CC) skeleton using a CVD method. This structure serves as a robust current collector for zinc plating. For example, to enhance the utilization of the conductive surface of CNTs, porous CNT networks were initially grown on carbon cloth (CC), which exhibited a high SSA and further electrodeposited zinc. The high conductivity and SSA of the CNT skeleton enabled low nucleation overpotential and created more uniform electric fields, leading to dendrite-free anodes (Fig. 7f). The coulombic efficiency was as high as 97–99% after undergoing multiple cycles at different current densities, which was superior to that of the Zn/CC anode in the same situation. In addition, the construction of a 3D CNT framework resulted in a more uniform electric field distribution on the electrode surface and significantly lower Zn nucleation overpotential, which was more conducive to the rapid migration and uniform nucleation of Zn^{2+} ions at the interface. Consequently, the Zn/CNT anode demonstrated outstanding electrochemical performance, achieving a high coulombic efficiency of 97.9% after 200 hours of cycling at deep discharge. The Zn//MnO_2 full battery exhibited excellent rate performance and high coulombic efficiency, with a capacity retention of 88.7% after 1000 long cycles (Fig. 7g). More importantly, the capacity retention was almost the same as that when the battery was flat under different bending conditions, demonstrating excellent mechanical flexibility (Fig. 7h).[33] Furthermore, zinc nanosheets (Zn NSs) could be electrodeposited onto CNT fibers, forming a Zn NSs@CNTF anode. This anode configuration offered copious active sites and an shortened ion diffusion path, which enhanced the reversible Zn/Zn^{2+} reaction kinetics and contributed to a prolonged cycling lifetime.[87]

The application of CNTs as host materials for zinc anodes in FZIBs not only enhances the electrochemical performance and mechanical flexibility of the batteries but also significantly extends their lifespan, indicating broad potential for future applications. Future research should concentrate on optimizing the structure and fabrication processes of carbon nanotubes to further improve the performance and commercial viability of FZIBs.

5.2. Graphene as a current collector or Zn host

5.2.1 Graphene as a current collector for cathodes. Graphene films are perfect for positive collectors owing to their

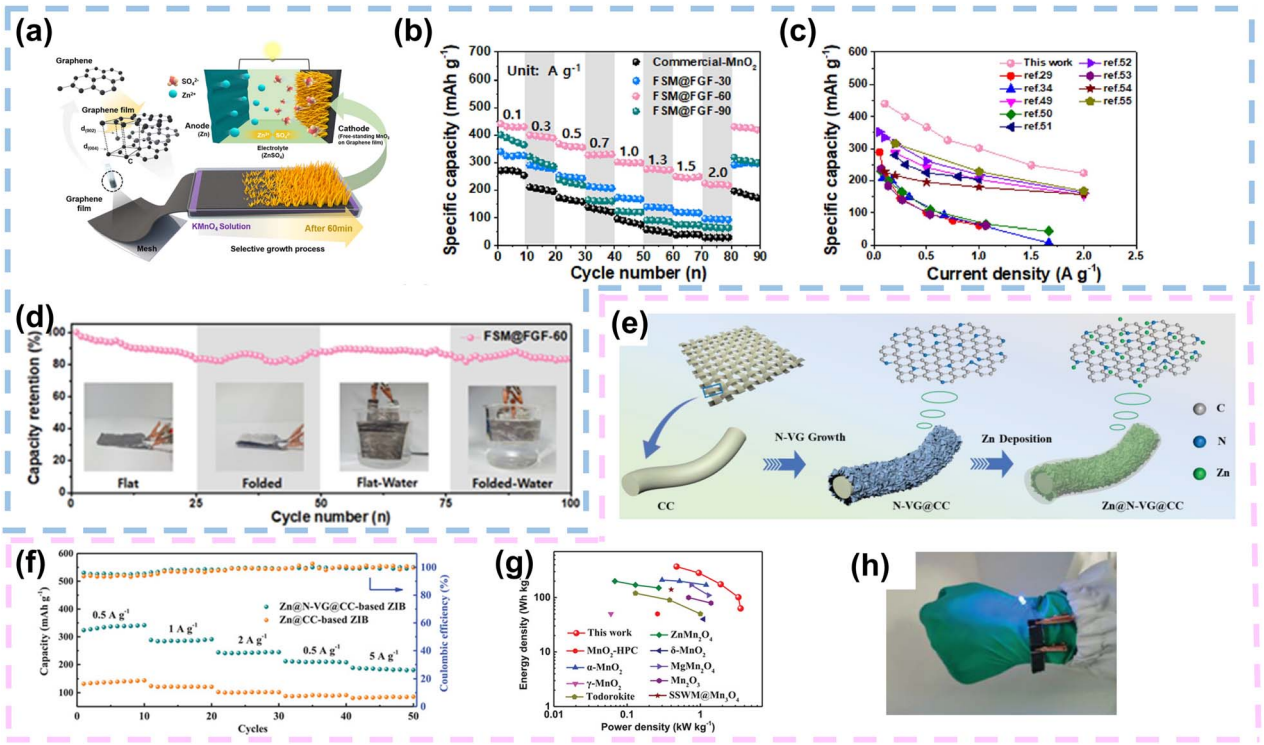

Fig. 8 Graphene as a current collector or Zn host in FZIBs. (a) Schematic illustration depicting the selective growth process of free-standing MnO_2 on a flexible graphene film for use as a binder-free cathode for FZIBs. (b) Comparative rate performances of commercial MnO_2, FSM@FGF-30, FSM@FGF-60, and FSM@FGF-90 at potential and current densities of 1.0–1.9 V and 0.1–2.0 A g^{-1}, respectively. (c) Comparative specific capacity, including those of previously reported ZIB materials. (d) Cycling performance of FSM@FGF for up to 100 cycles at a current density of 0.5 A g^{-1}. Reproduced with permission from ref. 90 Copyright 2022, Elsevier. (e) Schematic illustrations of preparing N-VG@CC and the Zn@N-VG@CC electrode. (f) Rate performance of the coin ZIBs based on Zn@CC and Zn@N-VG@CC anodes. (g) Ragone plot of the quasi-solid-state ZIB compared with other reported energy storage devices. (h) Flexible demonstration of two quasi-solid-state ZIBs connected in series. Reproduced with permission from ref. 92 Copyright 2021, Wiley.

high flexibility and superb electrical conductivity. Typical examples are shown in Fig. 8a, such as the direct growth of MnO_2 on flexible graphene films, which were successfully prepared by An's team through pouring graphene and PVDF solutions on stainless steel mesh. Additionally, the production of many oxygen-containing functional groups on the graphene surface from hydrochloric acid not only improved the wettability but also created numerous defects, which contributed to the smooth growth of MnO_2. Notably, graphene not only acted as a current collector to improve the electrical conductivity of MnO_2, but also promoted the independent growth of MnO_2 on graphene films without additives and binders. Owing to the application of binder-free electrodes and free-standing MnO_2 on the surface of the functionalized graphene film (denoted as FSM@FGF), FSM@FGF exhibited a rapid charge transfer process and uniform diffusion of zinc ions, which corresponded to an exceptional rate performance and remarkable cycling stability (Fig. 8b and c). The all-solid FZIBs, when assembled with gel electrolytes, showcased superior mechanical performance and water resistance. Notably, both in planar and folded states, the all-solid ZIBs exhibited superior cycling stability, regardless of the presence or absence of water (Fig. 8d).[90] Moreover, graphene could also serve as a lightweight collector to carry active materials due to its atomic-scale thickness and 2D structure, which facilitates self-assembly to form 2D films or 3D aerogels, thus enhancing the energy density of FZIBs. For instance, graphene could function as a 3D porous conductive support for 2D layered vanadium-based intercalated cathodes. Fan's team employed simple hydrothermal methods to generate zinc vanadate (ZOV) arrays with a thickness of less than 10 nm on the surface of graphene. The existence of the excellently flexible graphene conferred optimal mechanical performance to the ZOV cathode, where capacity retention was 96% after 100 repeated bends of the cathode even at a high mass loading of 4.1 mg cm^{-2}. Also with the adoption of lightweight graphene current collectors, the quasi-solid FZIB exhibited an energy density of 115 W h kg^{-1}, which was 200% higher than that of conventional current collectors like metal foil or carbon cloth.[91]

Graphene-based current collectors have been successfully employed in various cathode materials, including transition metal oxides, vanadium-based materials, and others. The use of graphene has resulted in batteries with higher energy densities, improved cycling stability, and enhanced rate performance compared to conventional current collectors. Future research in this area should focus on optimizing the synthesis and processing methods of graphene to further improve its electrical conductivity, mechanical properties, and compatibility with different cathode materials. Additionally, exploring new

graphene-based composite materials and hybrid structures could lead to further advancements in battery performance and applications. In conclusion, graphene-based current collectors hold great promise for improving the electrochemical performance and mechanical flexibility of cathodes in various battery applications, including portable electronics, electric vehicles, and energy storage systems. Continued research and development are expected to accelerate the commercialization of graphene-based battery technologies in the near future.

5.2.2 Graphene as a Zn host. Zinc foil is conventionally utilized as the anode material for FZIBs. Nevertheless, due to the growth of zinc dendrites and the inherent rigidity of zinc foil, the zinc anode typically exhibits poor mechanical performance and unsatisfactory rate performance. A new 3D flexible scaffold with highly conductive and flexible graphene construction for dendrite-free zinc metal anodes, which is considered as an effective method for constructing high performance composite zinc anodes. Cao *et al.* devised a two-step sequential CVD technique for the fabrication of nitrogen-doped vertical graphene (VG) nanosheets on carbon cloth. This substrate was initially prepared to serve as a flexible and conductive 3D framework, onto which zinc electrodeposition was performed. This innovative approach led to the synthesis of composite anodes (Zn@N-VG@CC) with exceptional performance characteristics, notably being dendrite-free (Fig. 8e). Owing to the zincophilic nature of the N atoms, the interaction between Zn^{2+} and the flexible carbon substrate could be efficiently enhanced, which brought a higher cycling performance and improved rate performance (Fig. 8f). Encouragingly, the quasi-solid-state ZIB exhibited the highest energy density of 371.24 W h kg^{-1} at a power density of at 0.474 kW kg^{-1}, which surpassed those reported for MnO_2-based ZIBs (Fig. 8g). Additionally, the two tandem ZIBs were mounted on the demonstrator's wrist to further test their wearable applications, maintaining their energy output for the LED without discomfort (Fig. 8h).[92] Moreover, graphene could be assembled with nano/micro-structured Zn powder and a film-forming agent to construct flexible Zn films as an alternative to commercial Zn foil. As a typical example, Niu *et al.* incorporated zinc microspheres with diameters of 3–5 μm into a composite film of SWCNTs and RGO using a similar blade coating process. In the Zn/SWCNTs–RGO film, zinc microspheres were evenly dispersed within a 3D conductive network formed by the SWCNTs and RGO sheets. The RGO sheets acted as hosts for the zinc microspheres, while the SWCNTs primarily played a dual role in enhancing the mechanical strength and conductivity of the composite film.[93]

In conclusion, graphene as a host material for zinc in ZIBs holds great promise for advancing the development of high-performance batteries with enhanced energy density, cycling stability, and safety. Continued research and innovation in this area is anticipated to hasten the adoption of graphene-based materials in next-generation energy storage technologies.

5.3. Carbon fibers as current collectors or Zn hosts

5.3.1 CFs as current collectors for cathodes. In recent years, CFs have been extensively utilized as promising current collectors in FZIBs due to their excellent electrical and thermal conductivity, high corrosion resistance, exceptional flexibility, lightweight nature, and cost-effectiveness. These CFs can be integrated into carbon cloth (CC) or assembled into carbon nanofiber membranes through electrospinning techniques.[111] In addition, *in situ* growth of nanostructured materials on carbon cloth not only strengthens the connection between the current collector and the active material without the need of a binder, but also enhances its electrical conductivity.[112,113] For example, Wang and his colleagues utilized a CVD method to fabricate a composite electrode of N-doped carbon nanosheets (N-CNSs) and MnO_2 on a CC substrate, assisted by a sacrificial MgO array template (CNSs@MnO_2) (Fig. 9a). The N-CNSs were uniformly and densely decorated on the CC surface, forming a cross-linked conductive network that provided a large SSA and facilitated rapid ion/electron transfer. Additionally, the robust N-CNSs substrate endowed the MnO_2 cathode and Zn anode (N-CNSs@Zn) with high mechanical stability, enabling the construction of advanced flexible Zn–MnO_2 batteries. As shown in Fig. 9b, the assembled N-CNSs@MnO_2//N-CNSs@Zn aqueous battery maintained 76.5% of its capacity retention at a high current density of 8.0 A g^{-1}. More importantly, our flexible quasi-solid-state N-CNSs@MnO_2//N-CNSs@Zn battery delivered a notable output voltage of 1.498 V in both normal and bent states (Fig. 9c).[94] Similarly, high-capacity layered VSe_2 nanosheets were synthesized on 1D N-CNFs through electrospinning, carbonization/oxidation, and salinization. The resulting core/shell nanostructures exhibited strong interfacial interaction, high mechanical flexibility, and excellent electrochemical properties. To further stabilize the composite structure and mitigate the dissolution of active materials during charge/discharge cycles, atomic layer deposition of Al_2O_3 layers was conducted uniformly over the VSe_2 nanosheets (Fig. 9d). This resulted in the formation of Al_2O_3@VSe_2 NSs@N-CNF films with an impressive tensile strength of 230 MPa. Notably, the flexible QAZIB, assembled with the Al_2O_3 VSe_2 NSs@N-CNF film as the cathode and Zn NSs@CNT film as the anode, demonstrated outstanding electrochemical performance (Fig. 9e and f). These FZIBs were capable of powering an integrated soft robot to walk on land and even in water, highlighting the multifunctionality of ZIBs and expanding the application fields of FZIBs.[95] In addition, Wu's team utilized a simple method of electrospinning and high-temperature calcination to combine V_2O_5 with carbon fiber cloth (CFC) to construct a V_2O_5-CFC electrode; the nanofiber structure of V_2O_5-CFC eased volume expansion during charge and discharge, while the 3D conductive network cross-linking of N-CNF facilitated electron transfer.[96]

Moreover, V_2O_3 nanoparticles (NPs) were embedded into carbon nanofibers by electrospinning to achieve V_2O_3@Carbon Nanofiber (V_2O_3@CNF) flexible binder-free ZIB cathode materials. The V_2O_3@CNF electrodes could withstand bending or twisting and exhibit excellent mechanical performance. After

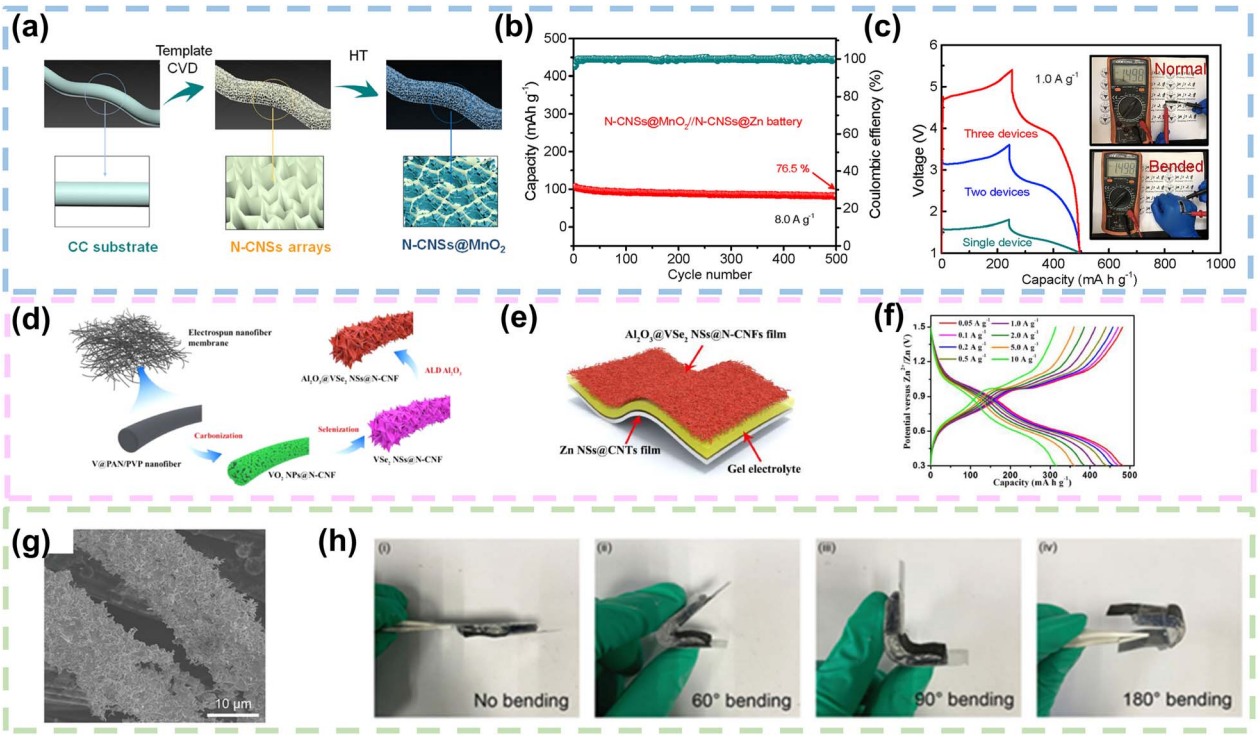

Fig. 9 CFs as current collectors or Zn hosts in FZIBs. (a) Schematic illustration preparation process of a flexible N-CNSs@MnO_2 cathode. (b) Cycling performance of the quasi-solid-state N-CNSs@MnO_2//N-CNSs@Zn battery at 8.0 A g^{-1}. (c) Galvanostatic charge/discharge curves obtained at a current density of 1.0 A g^{-1} for a single quasi-solid-state device and tandem devices consisting of two and three batteries units connected in series. Reproduced with permission from ref. 94 Copyright 2020, Elsevier. (d) Schematic illustration of the preparation process for the Al_2O_3@VSe_2 NSs@N-CNF film. (e) Schematic diagram illustration of the flexible QAZIB. (f) Galvanostatic charge/discharge curves of the flexible QAZIB at different current densities. Reproduced with permission from ref. 95 Copyright 2021, Elsevier. (g) SEM images of the Zn nanowires/CC anode. (h) Optical images of the self-healing flexible Zn-ion battery after bending to different angles. Reproduced with permission from ref. 100 Copyright 2021, Elsevier.

carbonization of the prepared V_2O_3@CNF cathode material, the pyridine and pyrrole N not only provided electrons to the π bond in the CNFs but also led to a number of structural defects, thus providing a large quantity of active sites. The V_2O_3@CNFs provided a superior specific capacity of 220 mA h g^{-1}, with a current density of 50 mA g^{-1}.[97] Moreover, Cao's group developed a MnO_2/CC hybrid electrode by modifying carbon cloth with zeolitic imidazolate frame-work-67 (ZIF-67). The carbon cloth substrate was enveloped by intricately arranged ultra-thin MnO_2 nanosheets, forming a distinctive hollow polyhedral structure. This MnO_2/CC electrode demonstrated a synergistic Zn^{2+} and H^+ co-intercalation mechanism, attributed to its exceptional reversibility. The substantial surface area of the MnO_2-loaded hollow polyhedron significantly enhanced electrolyte infiltration, mitigated volume expansion challenges, and concurrently promoted the conductivity of the underlying CC.[98]

The use of CFs as cathode current collectors in FZIBs presents a promising approach for improving the performance and durability of these energy storage devices. The integration of advanced materials and innovative fabrication techniques can lead to significant enhancements in electrochemical properties, mechanical flexibility, and overall battery efficiency, making CFs a valuable component in the development of next-generation flexible energy storage solutions.

5.3.2 CFs as current collectors or Zn hosts. In general, carbon fibers or carbon cloth can be utilized as lightweight, highly flexible conductive substrates to support zinc metal anodes. However, in order to reduce the surface energy, generally local and newly plated ions tend towards existing crystals, so that uniform deposition of Zn on the carbon cloth surface is not achieved, leading to the formation of zinc dendrites. To solve this problem, Chen and colleagues modified and uniformly grew MnO_2 films (MnO_2-utf) on carbon cloth, and the electrodeposition of CC@MnO_2-utf@Zn was conducted in a three-electrode system. There was no dendrite formation on the CC@MnO_2-utf@Zn anode because the MnO_2 films (MnO_2-utf) promoted the uniform deposition of Zn. In addition, MnO_2 as a common cathode material for ZIBs easily attracted Zn^{2+} through the intercalation mechanism, thus reducing the nucleation overpotential of Zn. Based on the above advantages, the CC@MnO_2-utf@Zn anode provided a specific capacity of 116.4 mA h g^{-1} at 2 A g^{-1} and excellent cycling performance after 300 repeated charging and discharging cycles with a high coulombic efficiency of 100% and a capacity retention rate of 81.0%.[99] In addition, to develop safe, portable, and wearable secondary battery systems, Zhang and his colleagues proposed novel self-healing FZIBs. This battery utilized a PVA/Zn $(CH_3COO)_2$/Mn $(CH_3COO)_2$ hydrogel as the electrolyte, VS_2 nanosheets grew on CC as the cathode, and

zinc nanowire-deposited CC as the anode. The SEM image of the electrochemically deposited Zn anode on CC was shown in Fig. 9g. The dense coating of zinc nanowires on the surface of the CFs formed a unified zinc nanowire/CC anode. The self-healing flexible battery demonstrated excellent mechanical performance when bent to 60°, 90°, and 180° (Fig. 9h).[100]

The scalability and versatility of CF-based zinc anode current collectors open new avenues for the advancement of next-generation flexible, stretchable, and customizable energy storage solutions. This approach not only enhances the performance and durability of ZIBs but also broadens their application potential in wearable electronics and other flexible devices.

6. Application of 1D/2D carbon materials in gel electrolytes

For the gel electrolyte of FZIBs, 1D/2D carbon materials can also be added as fillers into the gel electrolyte. Firstly, their large SSA and porous structure facilitate improved electrolyte–electrode interactions, enhancing ion transport kinetics and overall battery performance.[114–116] Secondly, the presence of functional groups on the surface of these carbon fillers can promote better adhesion between the electrolyte and the electrode interfaces, thereby enhancing the mechanical stability of the battery. Moreover, the addition of 1D/2D carbon materials can effectively inhibit the growth of dendrites during cycling, thus improving the long-term cycling stability and safety of FZIBs.[28] Overall, the utilization of these carbon fillers holds great promise for optimizing the gel electrolyte formulation and advancing the practical applications of FZIBs.[117]

Typically, 2D functional fillers provide great SSA, enabling increased number of active interfaces with polymers in composite polymer electrolytes (CPEs). GO, the most typical 2D filler, has been widely adopted in CPEs due to its numerous oxygen-containing functional groups. Specifically, GO possesses a long-range ordered monoatomic layer structure that is expected to create fast ion transport channels at the polymer–GO interface. Xiao *et al.* introduced GO as a filler into the $ZnSO_4$/$MnSO_4$-PVA-based gel electrolyte. As depicted in Fig. 10a, there were three main steps in the preparation of the GO-containing polymer hydrogel electrolyte (GPHE): (i) mixing PVA and GO, (ii) freeze/thaw processing, and (iii) $ZnSO_4$/$MnSO_4$ solution soaking. The molecular chain of PVA provided the framework for stiffness maintenance, while ions were transported within the $ZnSO_4$/$MnSO_4$ solution. In addition, a detailed finite element analysis (FEA) of the random distribution of GO in the GPHE was conducted using COMSOL Multiphysics, based on Monte

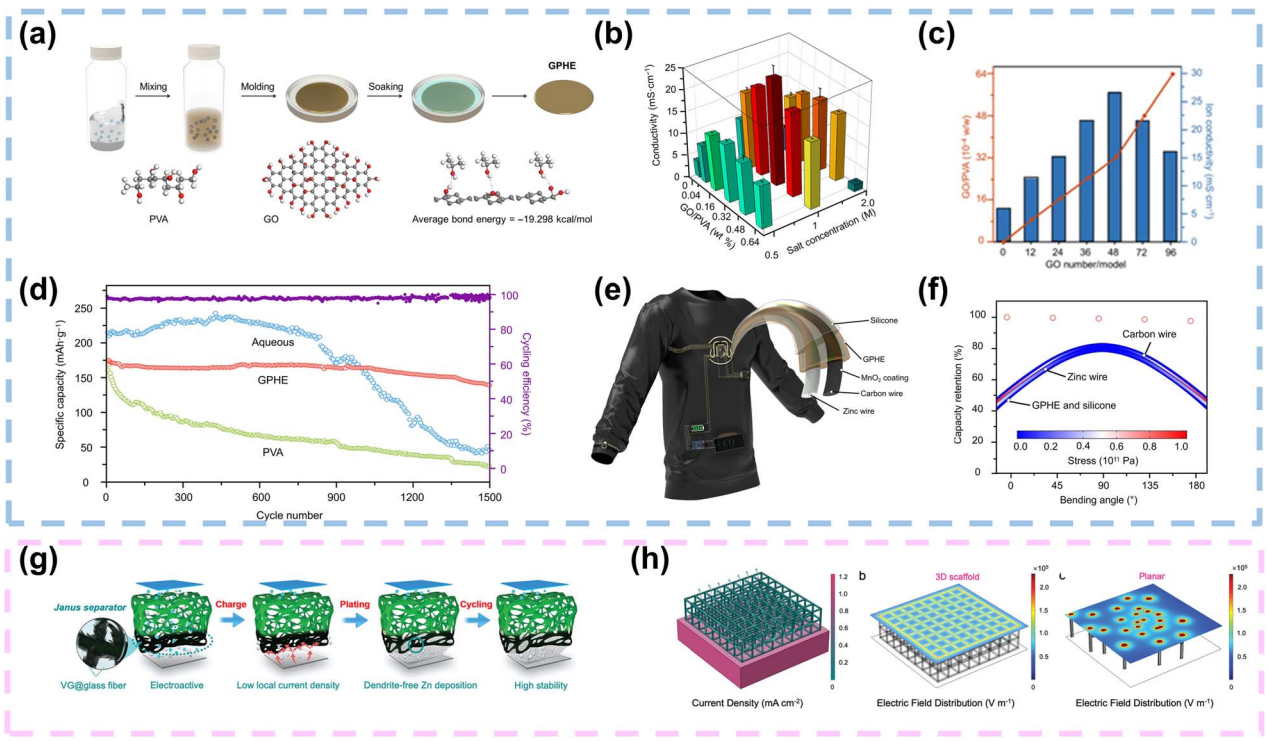

Fig. 10 Application of 1D/2D carbon materials in gel electrolytes and separators. (a) Schematic illustration of the preparation process of GPHE. (b) Measurement of ion conductivity of GPHEs with different PVA–GO mass ratios and soaking concentrations. (c) Calculation results of ion conductivity of GPHEs with different GO masses. (d) Cycling performance of coin cells with aqueous electrolyte, PVA electrolyte, and GPHE at a current density of 0.3 A g^{-1}. (e) Illustration and design of a flexible ZIB TBAN. (f) PHE-based ZIB fiber maintaining stable capacity output under different bending angles. The inset image shows bending stress and deformation of ZIB fibers. Reproduced with permission from ref. 31 Copyright 2021, AAAS. (g) A Janus separator employing a VG carpet directly grown on one side to reduce local current density and homogenize ion distribution. (h) Current distribution in the 3D scaffold. Electric field distribution of the Janus separator structure and pristine separator structure. Reproduced with permission from ref. 30 Copyright 2020, Wiley.

Carlo simulations. At high molecular weights, ion transport was primarily achieved through microscopic processes that were independent of the polymer length and viscosity (Fig. 10b). Moreover, the hydrogen bond formed between GO and the PVA polymer affected GO dispersion, enhancing ion mobility and forming a layered structure that bound molecularly to the PVA polymer. The resulting composite polymer electrolyte containing 0.32 wt% GO demonstrated favorable performance with an ionic conductivity of 21 mS cm^{-1} (Fig. 10c). A rechargeable solid-state zinc-ion fiber battery was developed, maintaining 98.0% capacity after over 1000 charging and discharging cycles (Fig. 10d). To demonstrate practical applications, the solid-state Zn/MnO_2 fiber battery successfully powered a textile-based active node (TBAN) for continuous monitoring of various physiological signals and wireless charging (Fig. 10e and f). The lightweight, low-cost, and high-performance Zn/MnO_2 fiber battery showed potential for mass production, highlighting its capability to power e-textiles for personalized healthcare.[31] Chen and co-workers fabricated V_2O_5/GO/PVA gel electrolytes with 5 wt% GO, which exhibited about a two orders of magnitude enhancement in mechanical performance compared with pure PVA gel electrolytes.[101] As mentioned above, 1D/2D carbon materials as fillers typically possess abundant functional groups. These groups can significantly enhance interactions with polymers and zinc salts, maximizing the anchoring of anions and reducing the affinity between zinc ions and polymers. This accelerates zinc ion transport and improves the compatibility at the filler–polymer interface.

7. Application of 1D/2D carbon materials in separators

Separators play a crucial role in battery systems by preventing direct contact between cathodes and anodes, thereby mitigating the risk of short circuits. Separator engineering, which includes modification and functionalization, has emerged as an innovative and effective strategy for developing high-performance energy storage devices.[118,119]

Typically, GF separators dominate in aqueous ZIBs due to their hydrophilic nature, high ionic conductivity, and porous structure. *In situ* modification of GF separators with conductive carbon materials, particularly graphene, presents a promising strategy to enhance electrochemical performance of ZIBs. Li *et al.* employed plasma-enhanced chemical vapor deposition (PECVD) to grow 3D VG carpets on one side of GF separators, creating Janus separators with an ample porous structure and large SSA to ensure uniform electric field distribution and reduced local current density. Additionally, the introduction of oxygen and nitrogen functional groups enhanced zincophilicity, regulating homogeneous Zn^{2+} fluxes and stabilizing Zn anodes (Fig. 10g). A simplified 3D model was constructed using the Janus separator structure, and as shown in Fig. 10h, the introduction of a 3D conductive VG scaffold significantly increased the surface area and effectively reduced the current density, outperforming 2D planar graphene. According to the 3D model, reducing the current density delayed the initiation of dendritic growth. The 3D VG scaffold provided a uniform electric field, facilitating the uniform deposition of Zn onto the VG framework. In contrast, the absence of a 3D scaffold in planar configurations easily triggered single nucleation points, leading to an uneven electric field which promoted the formation of Zn dendrites. Consequently, these robust Janus separators facilitated stable cycling of Zn//Zn symmetrical batteries for 300 hours at 0.5 mA cm^{-2} for 0.5 mA h cm^{-2}. Furthermore, $Zn//V_2O_5$ batteries achieved a high energy density of 182 W h kg^{-1} and withstood deformation without significant electrochemical decay.[30] Additionally, to achieve low-cost separators, Wu and colleagues proposed a functional cellulose nanofiber/graphene oxide (CG) separator. This separator featured abundant pores ranging from 10 to 50 nm, a smooth surface, and ample zincophilic oxygen-containing functional groups. These properties facilitated strong interactions with zinc, enabling uniform distribution of Zn^{2+} ions and promoting dendrite-free Zn anodes.[103]

While advancements have been notable, carbon separator research remains at an early stage. Presently, the prevalent GF separators suffer from fragility and large pores, prone to issues like zinc dendrite growth and short circuits.[120] Additionally, the separator/electrolyte and separator/electrode interface design has been overlooked, crucial for constructing FZIBs. To address this, an integrated system amalgamating all components into a single monolith could effectively stabilize interfaces and structures, ensuring resilience against deformations.

8. Conclusions and perspectives

This review provides a comprehensive summary of recent research advancements in 1D/2D carbon materials (carbon nanotubes, graphene, MXenes, and carbon fibers) for FZIBs. It mainly introduces the significant functions of these 1D/2D

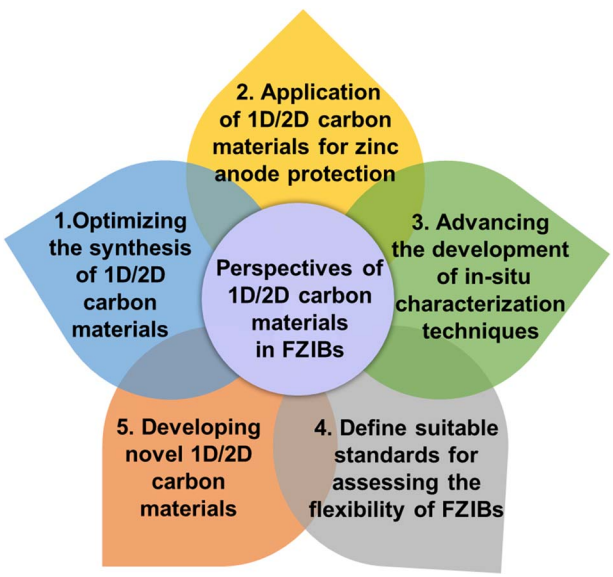

Fig. 11 Challenges and perspectives for future research on 1D/2D carbon materials in FZIBs.

materials as active materials, conductive networks, current collectors or Zn hosts in enhancing the performance of FZIBs. In the meantime, 1D/2D carbon materials are also widely applied in modified separators and gel electrolytes in FZIBs. In future commercial developments, 1D/2D carbon materials also demonstrate immense potential. Firstly, they can significantly enhance the energy density and cycling life of FZIBs, thereby meeting the market demand for high-performance batteries. Secondly, due to their superior mechanical flexibility, these materials can be used to develop various wearable devices and flexible electronic products, presenting new opportunities for the consumer electronics market. Despite the extensive progress in the research of 1D/2D carbon materials in FZIBs, there are still many unresolved issues which are discussed as follows (Fig. 11):

(1) Optimizing the synthesis of 1D/2D carbon materials. Precise synthesis methods allow for the creation of 1D/2D carbon materials with tailored structures and surface chemical properties to fulfill specific functional or component requirements. Although existing 1D/2D carbon materials generally meet the demands of high-performance energy storage devices, the unique structural and surface characteristics of 1D/2D carbon materials, such as high conductivity and hydrophilicity, assume crucial significance when considering the distinctions between FZIBs and other energy storage systems. In this context, precise modulation of the hydrophilic and hydrophobic nature of 1D/2D carbon materials becomes particularly pertinent.

(2) Application of 1D/2D carbon materials for zinc anode protection. Addressing the challenges posed by poor electrochemical and cycling stability of zinc metal anodes has driven researchers to predominantly focus on structural design of the zinc material. This involves modifying the zinc surface through the incorporation of supplementary protective layers, alongside optimizing the electrolyte composition. Within the context of 1D/2D carbon materials, which serve as both the core material and protective layer, the compatibility and intimate contact at the interfaces, namely the 1D/2D carbon material/zinc and/or 1D/2D carbon material/separators, emerge as critical factors for sustaining a stable microstructure and uniform zinc deposition. In essence, ensuring compatibility and close interaction at these interfaces is pivotal for stabilizing the microstructure and promoting homogeneous zinc deposition.

(3) Advancing the development of *in situ* characterization techniques. Currently, research on the energy storage mechanisms of zinc heavily relies on non-*in situ* characterization methods, which fall short in accurately revealing the dynamic changes in chemical composition, morphological evolution, oxidation states, and other factors of active materials under real experimental conditions. As a consequence, our understanding of the energy storage mechanisms of active materials and the continuous structural evolution of metal oxides during charge and discharge processes remains incomplete. Furthermore, a more profound investigation is required to discern the impact of introducing 1D/2D carbon materials on energy storage mechanisms. Moreover, a more detailed exploration of the interfacial interactions between 1D/2D carbon materials and metal oxides, as well as their effects on electrochemical performance, is necessary. To tackle these challenges, employing advanced *in situ* visualization and spectroscopic characterization techniques such as synchrotron X-ray absorption spectroscopy (XAS), transmission X-ray microscopy (TXM), X-ray photoelectron spectroscopy (XPS), transmission electron microscopy (TEM), and atomic force microscopy (AFM), plays an indispensable role in resolving these issues and gaining a deeper understanding of the role of 1D/2D carbon materials. Additionally, to achieve mass production of 1D/2D carbon materials, it is crucial to specifically consider costs. Some studies may opt for expensive raw materials, and complex testing techniques also constitute a significant portion of research expenses. Therefore, finding a relative balance between cost and outcomes could accelerate the process of commercial application.

(4) Define suitable standards for assessing the flexibility of FZIBs. Presently, the evaluation of conventional ZIBs typically encompasses parameters such as specific capacity, rate performance, cycling stability, energy density, and power density. Within this context, the discharge depth and current density significantly influence the cycling life of ZIBs. Furthermore, the validation of their exceptional flexibility often involves tests such as bending, twisting, and stretching in FZIBs. However, there currently exists a divergence in experimental methodologies and geometric parameters. This disparity hampers the progression of FZIBs. Consequently, it becomes essential to formulate a set of suitable standards to facilitate the smooth advancement and interdisciplinary application of FZIBs.

(5) Developing novel 1D/2D carbon materials. Although existing 1D/2D carbon materials have been widely used in many fields and have demonstrated great performance, the exploration of novel 1D/2D carbon materials is still an ongoing and evolving process. In addition, by focusing on green synthesis methods and utilizing renewable resources, researchers can minimize the environmental impact of producing 1D/2D carbon materials. Furthermore, it is essential to consider the end-of-life disposal and recyclability of 1D/2D carbon materials. Designing materials that are easily recyclable or biodegradable will ensure that their use does not lead to long-term environmental pollution. This approach aligns with the principles of a circular economy, promoting the reuse and recycling of materials to reduce waste and resource consumption. Integrating these considerations into the development of novel 1D/2D carbon materials will not only enhance their commercial viability but also support broader environmental and societal goals. By prioritizing safety and environmental impact alongside performance and cost, the next generation of 1D/2D carbon materials can meet the demands of both industry and the planet, paving the way for a sustainable energy future.

In conclusion, advanced 1D/2D carbon materials have made significant progress in enhancing the electrochemical performance of FZIBs. However, there are still challenges and limitations that require further research and resolution. The path ahead remains filled with challenges, necessitating ongoing efforts and exploration.

Data availability

This is a review paper. Data availability is not applicable to this article as no new data were created or analyzed in this study.

Conflicts of interest

There are no conflicts to declare.

Acknowledgements

The authors are grateful for financial support from the National Natural Science Foundation of China (Youth Program, No. 52204378 and No.22309209) and the Natural Science Foundation of Hunan province in China (Grant No. 2023JJ40709).

References

1 H. Huang, L. Han, J. Li, X. Fu, Y. Wang, Z. Yang, X. Xu, L. Pan and M. Xu, *J. Mater. Chem. A*, 2020, **8**, 10291–10300.
2 A. Sumboja, J. Liu, W. G. Zheng, Y. Zong, H. Zhang and Z. Liu, *Chem. Soc. Rev.*, 2018, **47**, 5919–5945.
3 C. Yoo, S. Lee, Y. Song, W. Chang, M. K. Park, Y. Ko and J. Cho, *Carbon Energy*, 2023, **5**, e335.
4 Y. Gao, L. Yu, J. C. Yeo and C. T. Lim, *Adv. Mater.*, 2020, **32**, e1902133.
5 H. R. Lim, H. S. Kim, R. Qazi, Y. T. Kwon, J. W. Jeong and W. H. Yeo, *Adv. Mater.*, 2020, **32**, e1901924.
6 W. Heng, S. Solomon and W. Gao, *Adv. Mater.*, 2022, **34**, e2107902.
7 J. He, N. Wang, Z. Cui, H. Du, L. Fu, C. Huang, Z. Yang, X. Shen, Y. Yi, Z. Tu and Y. Li, *Nat. Commun.*, 2017, **8**, 1172.
8 Y. M. J. H. Zhou, F. Wu, Y. T Hao, W. W. Ma, L. Li, M. Xie and R. J. Chen, *Angew. Chem., Int. Ed.*, 2023, **62**, e202304454.
9 Y. Du, Y. Li, B. B. Xu, T. X. Liu, X. Liu, F. Ma, X. Gu and C. Lai, *Small*, 2022, **18**, 2104640.
10 H. Li, L. Ma, C. Han, Z. Wang, Z. Liu, Z. Tang and C. Zhi, *Nano Energy*, 2019, **62**, 550–587.
11 X. Wang, L. Liu, Z. Hu, C. Peng, C. Han and W. Li, *Adv. Energy Mater.*, 2023, **13**, 2302927.
12 H. Lu, L. Liu, J. Zhang and J. Xu, *J. Colloid Interface Sci.*, 2022, **617**, 422–429.
13 Z. W. Hu, L. Y. Liu, X. Wang, Q. Q. Zheng, C. Han and a. W. J. Li, *Adv. Funct. Mater.*, 2024, 2313823.
14 H. Wang, K. Wang, E. Jing, M. Wei, J. Xiong, D. Zhong, Y. Zuo, B. Liang and P. Pei, *Energy Storage Mater.*, 2024, 103451.
15 J. Zhu, Z. Tie, S. Bi and Z. Niu, *Angew Chem. Int. Ed. Engl.*, 2024, e202403712.
16 L. Liu, H. Lu, C. Han, X. Chen, S. Liu, J. Zhang, X. Chen, X. Wang, R. Wang, J. Xu, H. K. Liu, S. X. Dou and W. Li, *ACS Nano*, 2023, **17**, 23065–23078.
17 H. Yu, D. Chen, Q. Li, C. Yan, Z. Jiang, L. Zhou, W. Wei, J. Ma, X. Ji, Y. Chen and L. Chen, *Adv. Energy Mater.*, 2023, **13**, 2300550.
18 L. Y. Liu, X. Y. Wang, Z. W. Hu, X. Wang, Q. Q. Zheng, C. Han, J. T. Xu, X. Xu, H. K. Liu, S. X. Dou and W. J. Li, *Angew. Chem., Int. Ed.*, 2024, e202405209.
19 Y. Song, W. Li, K. Zhang, C. Han and A. Pan, *Adv. Energy Mater.*, 2024, **14**, 2303352.
20 K. R. Ryan, M. P. Down, N. J. Hurst, E. M. Keefe and C. E. Banks, *eScience*, 2022, **2**, 365–381.
21 X. Meng, S. Zhou, J. Li, Y. Chen, S. Lin, C. Han and A. Pan, *Adv. Funct. Mater.*, 2023, **34**, 2309350.
22 J. Wu, Y. Wang, D. Deng, Y. Bai, M. Liu, X. Zhao, X. Xiong and Y. Lei, *J. Mater. Chem. A*, 2022, **10**, 19304–19319.
23 Y. Gao, C. Wang, H. Wang, C. Feng, H. Pan, Z. Zhang, J. He and Q. Wang, *Chem. Eng. J.*, 2023, **474**, 145446.
24 Y. Wang, Q. Li, H. Hong, S. Yang, R. Zhang, X. Wang, X. Jin, B. Xiong, S. Bai and C. Zhi, *Nat. Commun.*, 2023, **14**, 3890.
25 P. Ruan, S. Liang, B. Lu, H. J. Fan and J. Zhou, *Angew. Chem., Int. Ed.*, 2022, **61**, e202200598.
26 B. Huang, Z. Sun and G. Sun, *eScience*, 2022, **2**, 243–277.
27 W. Li, C. Han, Q. Gu, S. L. Chou, J. Z. Wang, H. K. Liu and S. X. Dou, *Adv. Energy Mater.*, 2020, **10**, 2303352.
28 K. Zhu, J. Luo, D. Zhang, N. Wang, S. Pan, S. Zhou, Z. Zhang, G. Guo, P. Yang, Y. Fan, S. Hou, Z. Shao, S. Liu, L. Lin, P. Xue, G. Hong, Y. Yang and Y. Yao, *Adv. Mater.*, 2024, e2311082.
29 H. Liu, Z. Xin, B. Cao, B. Zhang, H. J. Fan and S. Guo, *Advanced Science*, 2023, **11**, 2305806.
30 C. Li, Z. Sun, T. Yang, L. Yu, N. Wei, Z. Tian, J. Cai, J. Lv, Y. Shao, M. H. Rummeli, J. Sun and Z. Liu, *Adv. Mater.*, 2020, **32**, e2003425.
31 X. Xiao, X. Xiao, Y. H. Zhou, X. Zhao, G. R. Chen, Z. X. Liu, Z. H. Wang, C. Y. Lu, M. L. Hu, A. Nashalian, S. Shen, K. D. Xie, W. W. Yang, Y. J. Gong, W. B. Ding, P. Servati, C. Han, S. X. Dou, W. J. Li and J. Chen, *Sci. Adv.*, 2021, eabl3742.
32 W. Li, C. Han, K. Zhang, S. Chou and S. Dou, *J. Mater. Chem. A*, 2021, **9**, 6671–6693.
33 Y. Zeng, X. Zhang, R. Qin, X. Liu, P. Fang, D. Zheng, Y. Tong and X. Lu, *Adv. Mater.*, 2019, **31**, 1903675.
34 F. Gao, B. Mei, X. Xu, J. Ren, D. Zhao, Z. Zhang, Z. Wang, Y. Wu, X. Liu and Y. Zhang, *Chem. Eng. J.*, 2022, **448**, 137742.
35 F. Mo, G. Liang, Z. Huang, H. Li, D. Wang and C. Zhi, *Adv. Mater.*, 2020, **32**, e1902151.
36 K. K. Fu, J. Cheng, T. Li and L. Hu, *ACS Energy Lett.*, 2016, **1**, 1065–1079.
37 H. Dong, J. Li, J. Guo, F. Lai, F. Zhao, Y. Jiao, D. J. L. Brett, T. Liu, G. He and I. P. Parkin, *Adv. Mater.*, 2021, **33**, e2007548.
38 X. Li, D. Wang and F. Ran, *Energy Storage Mater.*, 2023, **56**, 351–393.
39 W. H. Wang, C. W. Li, S. Z. Liu, J. C. Zhang, D. J. Zhang, J. M. Du, Q. C. Zhang and Y. G. Yao, *Adv. Energy Mater.*, 2023, 2300250.
40 D. Wang, C. Han, F. Mo, Q. Yang, Y. Zhao, Q. Li, G. Liang, B. Dong and C. Zhi, *Energy Storage Mater.*, 2020, **28**, 264–292.

41 C. Tian, J. Wang, R. Sun, T. Ali, H. Wang, B. B. Xie, Y. Zhong and Y. Hu, *Angew. Chem., Int. Ed.*, 2023, **62**, e202310970.
42 L. Wu and Y. Dong, *Energy Storage Mater.*, 2021, **41**, 715–737.
43 Z. Liu, D. Wang, Z. Tang, G. Liang, Q. Yang, H. Li, L. Ma, F. Mo and C. Zhi, *Energy Storage Mater.*, 2019, **23**, 636–645.
44 P. Yu, Y. Zeng, H. Zhang, M. Yu, Y. Tong and X. Lu, *Small*, 2019, **15**, 1804760.
45 X. Zhong, Z. Zheng, J. Xu, X. Xiao, C. Sun, M. Zhang, J. Ma, B. Xu, K. Yu, X. Zhang, H. M. Cheng and G. Zhou, *Adv. Mater.*, 2023, **35**, e2209980.
46 L. Zhang, L. Chen, X. Zhou and Z. Liu, *Adv. Energy Mater.*, 2015, **5**, 550–587.
47 Y. Li, Z. Wang, Y. Cai, M. E. Pam, Y. Yang, D. Zhang, Y. Wang and S. Huang, *Energy Environ. Mater.*, 2022, **5**, 823–851.
48 X. Wang, C. Han, S. X. Dou and W. J. Li, *Nano Mater. Sci.*, 2022, DOI: **10.1016/j.nanoms.2022.10.004**.
49 C. Han, H. Li, A. Pan, S. Dou, Y. Liu, J. Liu and W. Li, *Chem. Eng. J.*, 2024, **481**, 148073.
50 Q. He, Z. Chang, Y. Zhong, S. Chai, C. Fu, S. Liang, G. Fang and A. Pan, *ACS Energy Lett.*, 2023, **8**, 5253–5263.
51 S. Liu, W. Liu, D. Ba, Y. Zhao, Y. Ye, Y. Li and J. Liu, *Adv. Mater.*, 2023, **35**, e2110423.
52 S. Huang, L. Hou, T. Li, Y. Jiao and P. Wu, *Adv. Mater.*, 2022, **34**, e2110140.
53 S. Li, Y. Liu, X. Zhao, Q. Shen, W. Zhao, Q. Tan, N. Zhang, P. Li, L. Jiao and X. Qu, *Adv. Mater.*, 2021, **33**, 2007480.
54 K. Shirvanimoghaddam, I. Ozen, P. Wu, S. Jafarzadeh, R. Yadav and M. Naebe, *Small Struct.*, 2024, 2300539.
55 F.-Z. Zhang, X.-B. Liu, C.-M. Yang, G.-D. Chen, Y. Meng, H.-B. Zhou and S.-H. Zhang, *Mater. Today*, 2024, **74**, 203–234.
56 J. A. Naveed, H. J. Yang, J. Yang, Y. N. Nuli and J. L. Wang, *Angew. Chem. Int. Ed.*, 2019, **58**, 2760–2764.
57 J. Zhou, M. Xie, F. Wu, Y. Mei, Y. Hao, L. Li and R. Chen, *Adv. Mater.*, 2022, **34**, e2106897.
58 S. Abdolhosseinzadeh, X. Jiang, H. Zhang, J. Qiu and C. Zhang, *Mater. Today*, 2021, **48**, 214–240.
59 N. Zhang, S. Huang, Z. Yuan, J. Zhu, Z. Zhao and Z. Niu, *Angew. Chem., Int. Ed.*, 2021, **60**, 2861–2865.
60 Y. Liu, Y. Jiang, Z. Hu, J. Peng, W. Lai, D. Wu, S. Zuo, J. Zhang, B. Chen, Z. Dai, Y. Yang, Y. Huang, W. Zhang, W. Zhao, W. Zhang, L. Wang and S. Chou, *Adv. Funct. Mater.*, 2020, **31**, 2008033.
61 C. Wan, J. Huang, K. Chen, C. Jiang, Q. Wu, P. Huang, Q. Xu, S. Qin and H. Xie, *Energy Storage Mater.*, 2024, **69**, 103384.
62 X. Chang, X. Cheng, H. Zhang, W. Li, L. He, X. Yin, X. Liu, J. Yu, Y. T. Liu and B. Ding, *Adv. Funct. Mater.*, 2023, **33**, 2215168.
63 G. Ge, Y. Wu, E. van der Heide, Z. Chen, J. Zhu and X. Zhuang, *J. Energy Storage*, 2024, **90**, 111900.
64 S. Zhai, N. Wang, X. Tan, K. Jiang, Z. Quan, Y. Li and Z. Li, *Adv. Funct. Mater.*, 2021, **31**, 2008894.
65 S. Pandiaraj, S. Aftab, G. Koyyada, F. Kabir, H. H. Hegazy and J. H. Kim, *Mater. Today Energy*, 2024, 101629.
66 X. Guan, Z. Li, X. Geng, Z. Lei, A. Karakoti, T. Wu, P. Kumar, J. Yi and A. Vinu, *Small*, 2023, **19**, e2207181.
67 B. Sun, N. Wang, X. Xie, L. Zhong, L. He, S. Komarneni and W. Hu, *J. Mater. Sci. Technol.*, 2025, **209**, 251–261.
68 D. Yuan, Y. Dou, Z. Wu, Y. Tian, K. H. Ye, Z. Lin, S. X. Dou and S. Zhang, *Chem. Rev.*, 2022, **122**, 957–999.
69 X. Wang, Y. Wang, Y. Jiang, X. Li, Y. Liu, H. Xiao, Y. Ma, Y. y. Huang and G. Yuan, *Adv. Funct. Mater.*, 2021, **31**, 2103210.
70 X. Li, M. Li, Q. Yang, H. Li, H. Xu, Z. Chai, K. Chen, Z. Liu, Z. Tang, L. Ma, Z. Huang, B. Dong, X. Yin, Q. Huang and C. Zhi, *ACS Nano*, 2020, **14**, 541–551.
71 S. Bi, Y. Wu, A. Cao, J. Tian, S. Zhang and Z. Niu, *Mater. Today Energy*, 2020, **18**, 100548.
72 Y. Du, X. Wang, Y. Zhang, H. Zhang, J. Man, K. Liu and J. Sun, *Chem. Eng. J.*, 2022, **434**, 134642.
73 J. Song, W. Wang, Y. Fang, S. Wang, D. He, R. Zhao and W. Xue, *Appl. Surf. Sci.*, 2022, **578**, 152053.
74 F. Wan, S. Huang, H. Cao and Z. Niu, *ACS Nano*, 2020, **14**, 6752–6760.
75 J. Zhang, Y. Huang, Z. Li, C. Gao, S. Jin, S. Zhang, X. Wang and H. Zhou, *Nanotechnology*, 2020, **31**, 375401.
76 X. Yue, H. Liu and P. Liu, *Chem. Commun.*, 2019, **55**, 1647–1650.
77 C. Gao, J. Wang, Y. Huang, Z. Li, J. Zhang, H. Kuang, S. Chen, Z. Nie, S. Huang, W. Li, Y. Li, S. Jin, Y. Pan, T. Long, J. Luo, H. Zhou and X. Wang, *Nanoscale*, 2021, **13**, 10100–10107.
78 A. Wang, W. Zhou, M. Chen, A. Huang, Q. Tian, X. Xu and J. Chen, *J. Colloid Interface Sci.*, 2021, **594**, 389–397.
79 Y. Huang, J. Liu, Q. Huang, Z. Zheng, P. Hiralal, F. Zheng, D. Ozgit, S. Su, S. Chen, P.-H. Tan, S. Zhang and H. Zhou, *npj Flex. Electron.*, 2018, **2**, 21.
80 J. Wang, J.-G. Wang, H. Liu, Z. You, Z. Li, F. Kang and B. Wei, *Adv. Funct. Mater.*, 2021, **31**, 2007397.
81 F. Wan, X. Wang, S. Bi, Z. Niu and J. Chen, *Sci. China Chem.*, 2019, **62**, 609–615.
82 F. Shi, C. Mang, H. Liu and Y. Dong, *New J. Chem.*, 2020, **44**, 653–657.
83 M. Shi, B. Wang, C. Chen, J. Lang, C. Yan and X. Yan, *J. Mater. Chem. A*, 2020, **8**, 24635–24644.
84 M. Qi, F. Li, Z. Zhang, Q. Lai, Y. Liu, J. Gu and L. Wang, *J. Colloid Interface Sci.*, 2022, **615**, 151–162.
85 Z. Shi, Q. Ru, Z. Pan, M. Zheng, F. Chi-Chun Ling and L. Wei, *Chemelectrochem*, 2021, **8**, 1091–1097.
86 M. Shi, B. Wang, Y. Shen, J. Jiang, W. Zhu, Y. Su, M. Narayanasamy, S. Angaiah, C. Yan and Q. Peng, *Chem. Eng. J.*, 2020, **399**, 135386.
87 Y. Lu, H. Zhang, H. Liu, Z. Nie, F. Xu, Y. Zhao, J. Zhu and W. Huang, *Nano Lett.*, 2021, **21**, 9651–9660.
88 X. Shen, X. Wang, Y. Zhou, Y. Shi, L. Zhao, H. Jin, J. Di and Q. Li, *Adv. Funct. Mater.*, 2021, **31**, 2101579.
89 K. Wang, X. Zhang, J. Hang, X. Zhang, X. Sun, C. Li, W. Liu, Q. Li and Y. Ma, *ACS Appl. Mater. Interfaces*, 2018, **10**, 24573–24582.
90 Y. G. Lee, J. Lee and G. H. An, *Chem. Eng. J.*, 2021, **414**, 128916.

91 D. Chao, C. R. Zhu, M. Song, P. Liang, X. Zhang, N. H. Tiep, H. Zhao, J. Wang, R. Wang, H. Zhang and H. J. Fan, *Adv. Mater.*, 2018, **30**, e1803181.
92 Q. Cao, H. Gao, Y. Gao, J. Yang, C. Li, J. Pu, J. Du, J. Yang, D. Cai, Z. Pan, C. Guan and W. Huang, *Adv. Funct. Mater.*, 2021, **31**, 2103922.
93 M. Yao, Z. Yuan, S. Li, T. He, R. Wang, M. Yuan and Z. Niu, *Adv. Mater.*, 2021, **33**, e2008140.
94 Y. Zhang, S. Deng, Y. Li, B. Liu, G. Pan, Q. Liu, X. Wang, X. Xia and J. Tu, *Energy Storage Mater.*, 2020, **29**, 52–59.
95 J. Yang, H. Yang, C. Ye, T. Li, G. Chen and Y. Qiu, *Energy Storage Mater.*, 2022, **46**, 472–481.
96 N. Xu, C. Yan, W. He, L. Xu, Z. Jiang, A. Zheng, H. Wu, M. Chen and G. Diao, *J. Power Sources*, 2022, **533**, 231358.
97 X. Liu, Z. Wang, Y. Niu, C. Liu, H. Chen, X. Ren, Z. Liu, W.-M. Lau and D. Zhou, *ACS Appl. Energy Mater.*, 2022, **5**, 3525–3535.
98 F. Wu, X. Gao, X. Xu, Y. Jiang, X. Gao, R. Yin, W. Shi, W. Liu, G. Lu and X. Cao, *Chemsuschem*, 2020, **13**, 1537–1545.
99 Y. Chen, J. Li, S. Zhang, J. Cui and M. Shao, *Adv. Mater. Interfaces*, 2020, **7**, 2196–7350.
100 J. Liu, J. Long, Z. Shen, X. Jin, T. Han, T. Si and H. Zhang, *Adv. Sci.*, 2021, **8**, 2004689.
101 R. G. Lv, H. Y. Wu, Z. H. Jiang, A. Y. Zheng, H. Y. Yu and M. Chen, *Electrochim. Acta*, 2022, 140998.
102 C. K. Liu, Y. Tian, Y. L. An, Q. L. Yang, S. L. Xiong, J. K. Feng and Y. T. Qian, *Chem. Eng. J.*, 2022, **430**, 132748.
103 J. Cao, D. Zhang, C. Gu, X. Wang, S. Wang, X. Zhang, J. Qin and Z. S. Wu, *Adv. Energy Mater.*, 2021, **11**, 2101299.
104 X. Xia, J. Yang, Y. Liu, J. Zhang, J. Shang, B. Liu, S. Li and W. Li, *Adv. Sci.*, 2022, e2204875.
105 X. Gao, H. Wu, C. Su, C. Lu, Y. Dai, S. Zhao, X. Hu, F. Zhao, W. Zhang, I. P. Parkin, C. J. Carmalt and G. He, *Energy Environ. Sci.*, 2023, **16**, 1364–1383.
106 X. Gao, C. Shen, H. Dong, Y. Dai, P. Jiang, I. P. Parkin, H. Zhang, C. J. Carmalt and G. He, *Energy Environ. Sci.*, 2024, **17**, 2287–2297.
107 M. Naguib, M. Kurtoglu, V. Presser, J. Lu, J. Niu, M. Heon, L. Hultman, Y. Gogotsi and M. W. Barsoum, *Adv. Mater.*, 2011, **23**, 4248–4253.
108 M. Naguib, V. N. Mochalin, M. W. Barsoum and Y. Gogotsi, *Adv. Mater.*, 2014, **26**, 992–1005.
109 J. Zheng, J. A. Lochala, A. Kwok, Z. D. Deng and J. Xiao, *Adv. Sci.*, 2017, **4**, 1700032.
110 J. Shin, J. Lee, Y. Park and J. W. Choi, *Chem. Sci.*, 2020, **11**, 2028–2044.
111 S. Yang, Y. Cheng, X. Xiao and H. Pang, *Chem. Eng. J.*, 2020, **384**, 123294.
112 J. Xu, Z. Dong, K. Huang, L. Wang, Z. Wei, L. Yu and X. Wu, *Scr. Mater.*, 2022, **209**, 114368.
113 Y. Zhuang, Y. Xie, B. Fei, D. Cai, Y. Wang, Q. Chen and H. Zhan, *J. Mater. Chem. A*, 2021, **9**, 21313–21322.
114 L. Chen, T. Xiao, J. L. Yang, Y. Liu, J. Xian, K. Liu, Y. Zhao, H. J. Fan and P. Yang, *Angew. Chem., Int. Ed.*, 2024, e202400230.
115 Q. Liu, Z. Yu, Q. Zhuang, J. K. Kim, F. Kang and B. Zhang, *Adv. Mater.*, 2023, **35**, e2300498.
116 Y. Zhang, L. Zhao, Y. Liang, X. Wang and Y. Yao, *eScience*, 2022, **2**, 110–115.
117 H. Xia, G. Xu, X. Cao, C. Miao, H. Zhang, P. Chen, Y. Zhou, W. Zhang and Z. Sun, *Adv. Mater.*, 2023, **35**, e2301996.
118 W. Zhou, M. Yang, M. Chen, G. Zhang, X. Han, J. Chen, D. Ma and P. Zhang, *Adv. Funct. Mater.*, 2024, 2315444.
119 F. Shen, H. Du, H. Qin, Z. Wei, W. Kuang, N. Hu, W. Lv, Z. Yi, D. Huang, Z. Chen and H. He, *Small*, 2024, **20**, e2305119.
120 L. Wu, Y. Zhang, P. Shang, Y. Dong and Z.-S. Wu, *J. Mater. Chem. A*, 2021, **9**, 27408–27414.

